

ANISOTROPIC COMPACT STARS IN THE MIMETIC GRAVITATIONAL THEORY

G. G. L. NASHED¹

¹*Centre for theoretical physics, the British University in Egypt, 11837 - P.O. Box 43, Egypt*

ABSTRACT

In this paper, we consider the mimetic gravitational theory to derive a novel category of anisotropic star models. To end and to put the resulting differential equations into a closed system, the form of the metric potential g_{rr} as used by Tolman (Tolman 1939) is assumed as well as a linear form of the equation-of-state. The resulting energy-momentum components, energy-density, and radial and tangential pressures contain five constants; three of these are determined through the junction condition, matching the interior with the exterior Schwarzschild solution the fourth is constrained by the vanishing of the radial pressure on the boundary and the fifth is constrained by a real compact star. The physical acceptability of our model is tested using the data of the pulsar 4U 1820-30. The stability of this model is evaluated using the Tolman-Oppenheimer-Volkoff equation and the adiabatic index and it is shown to be stable. Finally, our model is challenged with other compact stars demonstrating that it is consistent with those stars.

Keywords: Mimetic gravitational theory – spherically symmetric interior solution – TOV – stability – Adiabatic index.

1. INTRODUCTION

Inflation has achieved remarkable success in solving some of the most important cosmic puzzles, such as the problem of flatness, the problem of the horizon, and the problems of fine-tuning (Guth 1981; Albrecht & Steinhardt 1982; Linde 1982). Furthermore, it has also been declared that if the pre-inflationary density fluctuations are allowed to grow very largely over a short time ($\sim 10^{-33}$ sec.), a clear and systematic explanation of the construction of the large-scale and anisotropic cosmic microwave background structures is supplied (Mukhanov & Chibisov 1981; Guth & Pi 1982; Hawking 1982; Starobinsky 1982).

In Einstein's general relativity (GR), the scalar field which is coined as "inflaton" is responsible for executing inflation (Mukhanov & Chibisov 1981). In the GR realm, many studies have been carried out that have confirmed the consistency of the scalar with observations (Hossain et al. 2014; Martin et al. 2014a,b; Geng et al. 2015; Huang et al. 2016). However, GR still faces many challenges in confronting the accelerated expansion of our universe, among others, which is supported by observational data (Riess et al. 1998, 2004; Perlmutter et al. 1999; Ade et al. 2016). Modified gravitational theories are considered as being reliable in identifying cosmic problems such as the flat spin curves of spiral galaxies or the late cosmic acceleration, without the need for dark matter and dark energy (Capozziello & De Laurentis 2011; Nojiri & Odintsov 2011; Nashed 2007; Nojiri et al. 2017; De Felice & Tsujikawa 2010). Modified gravitational theories lead to scale-dependent interactions and preserve the results of Einstein's theory at scales of the solar system (Capozziello & De Laurentis 2011).

Another modified gravitational theory that has aimed to investigate dark matter is the mimetic dark matter model that was built by Chamseddine and Mukhanov (Chamseddine & Mukhanov 2013). They constructed a model whose concept was based on the isolation of the scalar degree-of-freedom of the metric. This model was able to predict dark matter as well as dark energy (Chamseddine et al. 2014) and many cosmological solutions (Chamseddine et al. 2014) that resolve singularities (Chamseddine & Mukhanov 2017a,b) and construct a ghost-free massive gravity model (Chamseddine & Mukhanov 2018).

The construction of the mimetic theory can be investigated as a specific form of conformal transformation in which the new metrics, as well as the old ones are degenerate. The use of non-singular conformal transformation produces an increase in the number of degrees-of-freedom, and thus; the longitudinal sector of gravity turns out to be dynamic (Deruelle & Rua 2014; Domnech et al. 2015; Firouzjahi et al. 2018; Shen et al. 2019; Gorji et al. 2020). Generally, conformal transformation means a relation between $g_{\alpha\beta}$, which is considered the physical one, to $\bar{g}_{\alpha\beta}$, which is the auxiliary metric, and ζ , which is the scalar field,

through the following transformation:

$$g_{\alpha\beta} = -(\bar{g}_{\mu\nu}\partial^\mu\zeta\partial^\nu\zeta)\bar{g}_{\alpha\beta}. \quad (1)$$

The above transformation gives the following constraint (Gorji et al. 2020)

$$g^{\alpha\beta}\partial_\alpha\zeta\partial_\beta\zeta = -1. \quad (2)$$

Therefore, $\partial_\alpha\zeta$ is a space such that we consider the positive sign and a time-like such that we consider the negative sign. The famous mimetic theory is that with a negative sign, and in this study, the positive sign is dealt with an extension to the mimetic gravitational theory (MGT). Equation (1) tells us that we cannot write $\bar{g}_{\alpha\beta}$ in terms of $g_{\alpha\beta}$ since it is non-invertible (Deruelle & Rua 2014). The extra degree of freedom linked to the transformation (1) accounts for the longitudinal sector of gravity. Starting with the Einstein-Hilbert action that contains the physical metric $g_{\alpha\beta}$ and carries out the transformation (1) $g^{\alpha\beta}$ and ζ which are dynamic scalar fields (Chaichian et al. 2014).

Generally, when studying compact stars a spherically symmetric spacetime that has isotropy can be supposed. The isotropy and homogeneity of astrophysical compact stellar objects cannot be considered as the general physical characteristics of these stellar objects; even though they could supply us with some solvable features. This is because the fluid pressure can be considered to have two different components that provide the anisotropy, $\Delta = p_t - p_r$. Such a case is called inhomogeneous where the source of the inhomogeneity results from the tangential, p_t , and the radial, p_r , pressures therefore, the distribution of matter is not in isotropic form. The idea of anisotropy was first considered by (Ruderman 1972) and then by many researchers (Canuto 1974; Bowers & Liang 1974; Herrera & Santos 1997). Currently, the source of anisotropy can be thought of as being due to different factors:

- Superfluid 3A,
- a core of the region where the density is very high,
- a mixture of fluids of different types,
- different condensate states,
- relativistic particles in the compact stars
- phase transition,
- rotational motion,
- and the existence of the magnetic field, among others (Ivanov 2002; Varela et al. 2010; Rahaman et al. 2012; Kalam et al. 2012; Deb et al. 2018; Shee et al. 2016; El Hanafy & Nashed 2016; Maurya et al. 2016, 2018; Deb et al. 2017).

This study aims to derive an interior spherically symmetric solution in the frame of MGT and to test if this solution represents a true compact star.

The structure of this research is as follows: In Section 2, the cornerstone of MGT is given and its field equations are derived. In Section 3, the field equations of MGT are applied to a spherically symmetric line element that has two unknown functions. To close the system of differential equations, we assume the metric potential g_{rr} to have the form given by Tolman (Tolman 1939), and assume a linear form of the equation-of-state (EoS) between the density and radial pressures. In Section 4, the necessary requirements that any true compact star should satisfy are stated. In Section 5, the physical properties of our model are given, showing that the metric potential and the energy-momentum components are well defined in the center of the star. Because our model has five constants of integration, we made a junction condition with an exterior solution, a Schwarzschild solution, and assumed that the radial pressure vanishes at the boundary of the star. From these constraints and the use of the radial EoS four constants are determined leaving the fifth one to be constrained by the comparison with the true star. In Section 6, the mass and radius of the compact star 4U 1820-30, are used showing that our model satisfies all the conditions required for any true compact star. In Section 7 the Tolman-Oppenheimer-Volkoff (TOV) equation and the adiabatic index of our model are derived and the model's willingness to be stable is shown. Also, in Section 7, other compact stars are studied and their relevant constants are derived, with these results being summarized in Tables (1) and (2). In Section 8, the results of the present study are summarized.

2. BRIEF SUMMARY OF THE MIMETIC GRAVITATIONAL THEORY

The term ‘‘mimetic dark matter’’ was proposed in the literature by Mukhanov and Chamseddine (Chamseddine et al. 2014) however, such a term was already known in the theories of papers written at earlier times (Lim et al. 2010; Gao et al. 2011; Capozziello et al. 2010; Sebastiani et al. 2017). The Lagrangian of the mimetic theory in four-dimensions takes the following form:

$$\mathcal{L} := \frac{1}{2\chi} \int d^4x \sqrt{-g(\bar{g}_{\mu\nu}, \zeta)} R(\bar{g}_{\mu\nu}, \zeta) - \int d^4x \sqrt{-g(\bar{g}_{\mu\nu}, \zeta)} \mathcal{L}_m, \quad (3)$$

where χ is the gravitational constant, $\chi = \frac{8\pi G}{c^4}$, G is the Newtonian constant, c is the speed of light, $g(\bar{g}_{\mu\nu}, \zeta)$ is the determinant of the metric tensor, ζ is the scalar field, R is the Ricci scalar, and \mathcal{L}_m is the Lagrangian of matter. Using Eq. (3) the field equations

of the MGT can be obtained as follows:

$$G_{\mu}^{\nu} - (G - T)\partial_{\mu}\zeta\partial^{\nu}\zeta = \chi T_{\mu}^{\nu}, \quad \nabla_{\mu} [(G - T)\partial^{\mu}\zeta] = 0, \quad (4)$$

where, $G_{\mu\nu}$ and $T_{\mu\nu}$ are the Einstein and stress energy tensors and G and T are their traces with $G = -R$. The stress-energy tensor, T_{μ}^{ν} , is the energy-momentum tensor for fluids whose configuration has anisotropy and it is represented by:

$$T_{\mu}^{\nu} = (p_t + \rho)u_{\mu}u^{\nu} + p_t\delta_{\mu}^{\nu} + (p_r - p_t)\xi_{\mu}\xi^{\nu}, \quad (5)$$

where u_{μ} is the time-like vector defined as $u^{\mu} = [1, 0, 0, 0]$ and ξ_{μ} is the unit radial vector with its space-like property, defined by $\xi^{\mu} = [0, 1, 0, 0]$ such that $u^{\mu}u_{\mu} = -1$ and $\xi^{\mu}\xi_{\mu} = 1$.

This study aims to apply the field equations (4) to a spherically symmetric spacetime.

3. INTERIOR SOLUTION IN MIMETIC THEORY

In this section, the field equations of MGT, Eq. (4), are to be applied to a spherically symmetric spacetime. For this purpose we use the following metric:

$$ds^2 = w(r)dt^2 - w_1(r)dr^2 - r^2 (d\theta^2 + \sin^2\theta d\phi^2), \quad (6)$$

where $w(r)$ and $w_1(r)$ are unknown functions. By applying the field equations (4) to the spacetime (6), we obtain the following non-linear differential equations:

$$\begin{aligned} \frac{w_1' r + w_1^2 - w_1}{w_1^2 r^2} &= 8\pi\rho, \\ \frac{1}{2w_1^3 r^2 w^2} &\left(2w'r w w_1^2 - 2w_1^3 w^2 + 2w^2 w_1^2 + \zeta'^2 \left[\pi(16r^2 w^2 w_1^2 \rho - 16r^2 w^2 w_1^2 p_r - 32r^2 w^2 w_1^2 p_t) - 4w_1' r w^2 \right. \right. \\ &\left. \left. - 4w^2 w_1^2 + 4w^2 w_1 + 4w'r w w_1 - r^2 w' w_1' w + 2r^2 w'' w w_1 - r^2 w'^2 w_1 \right] \right) = -8\pi p_r, \\ \frac{2w_1' w^2 - 2w' w w_1 + r w' w_1' w - 2r w'' w w_1 + r w'^2 w_1}{4r w^2 w_1^2} &= -8\pi p_t. \end{aligned} \quad (7)$$

where $w \equiv w(r)$, $w_1 \equiv w_1(r)$, $\zeta \equiv \zeta(r)$, and $'$ is the ordinary derivative, i.e., $w' \equiv \frac{dw}{dr}$. The above differential system consists of three independent equations in six unknown functions; w , w_1 , ρ , p_r , p_t , and ζ . Therefore, three extra conditions are required to solve the aforementioned system. One of these conditions is to assume the metric potential g_{rr} to have the form:

$$w_1 = 1 + s_1 r^2 + s_2 r^4, \quad (8)$$

where s_1 and s_2 are constants to be determined from the matching conditions. The metric potential (8) was proposed by Tolman (1939) to model realistic compact stellar objects. Interestingly, the same metric component is used to describe relativistic anisotropic stellar objects with a prescribed linear EoS of the form:

$$p_r = s_3 \rho + s_4, \quad (9)$$

where s_3 and s_4 are constants. Finally, to satisfy Eq. (2) we assume the scalar field in the form:

$$\zeta = \int \frac{1}{\sqrt{w_1}} dr. \quad (10)$$

Using Eq. (8) in the first equation of (7) we obtain the form of the density; then, using this form with Eq. (10) in the remainder of Eqs. (7) and (9) we obtain the form of w as follows:

$$w = s_5 \left(1 + s_1 r^2 + s_2 r^4 \right)^{s_3} e^{\frac{r^2 \left(16\pi s_2 s_4 r^4 + 24\pi s_1 s_4 r^2 + 3s_2 s_3 r^2 + 3s_2 r^2 + 6\pi s_3 s_1 + 48s_4 + 6s_1 \right)}{12}}. \quad (11)$$

Consequently, the physical quantities are obtained as

$$\rho(r) = \frac{s_2^2 r^6 + 2s_1 s_2 r^4 + (5s_2 + s_1^2) r^2 + 3s_1}{8\pi \left(1 + s_1 r^2 + s_2 r^4 \right)^2},$$

$$p_r(r) = \frac{1}{8\pi (1 + s_1 r^2 + s_2 r^4)^2} \left[8\pi s_2^2 s_4 r^8 + (s_2^2 s_3 + 16\pi s_1 s_2 s_4) r^6 + (8\pi s_1^2 s_4 + 16\pi s_2 s_4 + 2 s_1 s_2 s_3) r^4 + (5 s_2 s_3 + s_1^2 s_3 + 16\pi s_1 s_4) r^2 + 3 s_1 s_3 + 8\pi s_4 \right], \quad (12)$$

where we give the form of the tangential pressure and the anisotropic force in Appendix A. It is important to mention that the anisotropic force is defined as $\frac{2\Delta}{r}$ and it is attractive if $p_r - p_t > 0$ and will be repulsive if $p_r - p_t < 0$. The mass contained within a radius r of the sphere is defined as:

$$m(r) = \int_0^r \rho(\eta) \eta^2 d\eta. \quad (13)$$

Using Eq. (12) in Eq. (13), we get

$$m(r) = \frac{r^3 (s_1 + s_2 r^2)}{16\pi (1 + s_1 r^2 + s_2 r^4)}. \quad (14)$$

The compactness parameter of a spherically symmetric source with radius r takes the form (Singh et al. 2019)

$$u(r) = \frac{r^2 (s_1 + s_2 r^2)}{16\pi (1 + s_1 r^2 + s_2 r^4)}. \quad (15)$$

In the next section, we will state the physical requirements that any viable stellar structure must satisfy and ascertain whether the model (12) with the form of tangential pressure given in Appendix A satisfies them.

4. REQUIREMENTS FOR A PHYSICALLY CONSISTENT STELLAR MODEL

Any physical viable stellar model must satisfy the following conditions throughout the stellar configurations:

- ◊ The gravitational metric potentials, $w(r)$ and $w_1(r)$, and the components of the energy-momentum tensor ρ , p_r , p_t must be well-defined at the center of the star, as well as being regular and free from singularity throughout the interior of the star.
- ◊ The density, ρ , must be positive in the interior of the stellar model, i.e., $\rho \geq 0$. The value of the density at the center of the star should be positive, finite and monotonically decreasing toward the boundary.
- ◊ The radial and the tangential pressures must be positive inside the configuration of the fluid i.e., $p_r \geq 0$, $p_t \geq 0$. Also, the derivative of the density and the pressures must be negative, i.e., $\frac{d\rho}{dr} < 0$, $\frac{dp_r}{dr} < 0$ and $\frac{dp_t}{dr} < 0$. The radial pressure, p_r , must vanish at the boundary of the stellar model $r = \mathcal{R}$, however, the tangential pressure, p_t , need not be zero at the boundary. Finally, at the center of the star the pressures should be equal meaning that the anisotropy vanishes, i.e., $\Delta(r=0) = 0$.
- ◊ Any anisotropic fluid sphere must fulfill the following energy condition inequalities:
 - (i) Null energy condition (NEC): $p_r + \rho > 0$, $\rho > 0$.
 - (ii) Strong energy condition (SEC): $p_r + \rho > 0$, $p_t + \rho > 0$, $\rho - p_r - 2p_t > 0$.
 - (iii) Weak energy condition (WEC): $p_r + \rho > 0$, $\rho > 0$.
 - (iv) Dominant energy condition (DEC): $\rho \geq |p_r|$ and $\rho \geq |p_t|$.
- ◊ The interior metric potentials must join smoothly with the Schwarzschild exterior metric at the boundary.
- ◊ For a stable configuration, the adiabatic index must be greater than $\frac{4}{3}$.
- ◊ According to Herrera, the stability of the anisotropic stars should satisfy $0 > v_r^2 - v_t^2 > -1$ where v_r and v_t are the radial and transverse speeds respectively (Herrera 1992).
- ◊ To obtain a realistic model, the causality condition must be satisfied meaning that the speed of sound must be less than 1 (providing the speed of light $c = 1$) in the interior of the star, i.e., $1 \geq \frac{dp_r}{dr} \geq 0$, $1 \geq \frac{dp_t}{dr} \geq 0$.

We are now ready to analyze the aforementioned necessary physical conditions to test whether our model satisfies them.

5. PHYSICAL PROPERTIES OF THE MODEL

Let us test the model (12) and (A), see if it is consistent with realistic stellar structures. For this aim, the following topics need to be discussed:

5.1. The non-singular model

i- The metric potentials of this model satisfy:

$$w(0) = s_5 \quad \text{and} \quad w_1(0) = 1. \quad (16)$$

Equation (16) implies that the gravitational metric potentials are finite at the center of the configuration of the stellar model. Furthermore, the derivatives of these potentials are finite at the center, i.e., $w'_{r=0} = w'_{1r=0} = 0$. The aforementioned conditions ensure that the metric is regular at the center and behaves well throughout the interior of the stellar model.

ii-Density, radial, and tangential pressures; at the center, have the form:

$$\rho(0) = \frac{3s_1}{8\pi}, \quad p_r(0) = p_t(0) = \frac{3s_1s_3 + 8\pi s_4}{8\pi}. \quad (17)$$

Eq. (17) shows that the density is always positive if $s_1 > 0$, and the anisotropy is vanishing at the center. The radial and tangential pressures have positive values if $s_4 + \frac{3s_1s_3}{8\pi} > 0$; otherwise, they become negative. Furthermore, the Zeldovich condition (Zeldovich & Novikov 1971) states that the radial pressure must be less than or equal to the density at the center i.e., $\frac{p_r(0)}{\rho(0)} \leq 1$. Using the Zeldovich condition in Eq. (17), we obtain:

$$s_1 \leq \frac{3s_1s_3 + 8\pi s_4}{3}. \quad (18)$$

iii-The derivative of the energy density, radial, and tangential pressures of the model are, respectively:

$$\rho' = -\frac{r \left(12 s_2^2 r^4 + 3 r^6 s_2^2 s_1 + r^8 s_2^3 + 13 s_1 r^2 s_2 + 3 r^4 s_2 s_1^2 - 5 s_2 + 5 s_1^2 + r^2 s_1^3 \right)}{4\pi \left(1 + s_1 r^2 + s_2 r^4 \right)^3},$$

$$p'_r = s_3 \rho', \quad (19)$$

where $\rho' = \frac{d\rho}{dr}$, $p'_r = \frac{dp_r}{dr}$ and the form of $p'_t = \frac{dp_t}{dr}$ is given in Appendix B. Eqs. (19) and (B) show that the gradients of the density, radial, and tangential pressures are negative as will be shown in their plotting.

iv-The radial and tangential velocities of sound ($c = 1$) are obtained as:

$$v_r^2 = \frac{dp_r}{d\rho} = s_3, \quad (20)$$

where the form of tangential speed is given in Appendix C.

5.2. Matching conditions

We assume that the exterior spacetime of a non-rotating star is empty and is described by the exterior Schwarzschild solution that is given by the following form:

$$ds^2 = -\left(1 - \frac{2M}{r}\right) dt^2 + \left(1 - \frac{2M}{r}\right)^{-1} dr^2 + r^2 d\Omega^2, \quad (21)$$

where M is the total mass and $r > 2M$. It is necessary to match the interior spacetime metric (8) and (11) with the exterior Schwarzschild spacetime metric (21) at the boundary of the star where $r = \mathcal{R}$. The continuity of the metric functions across the boundary $r = \mathcal{R}$ gives the conditions

$$w(r = \mathcal{R}) = \left(1 - \frac{2M}{\mathcal{R}}\right), \quad w_1(r = \mathcal{R}) = \left(1 - \frac{2M}{\mathcal{R}}\right)^{-1}. \quad (22)$$

Furthermore, we use the fact that the radial pressure approaches zero at a finite value of the radial parameter r that coincides with the radius of the star \mathcal{R} . Therefore, the radius of the star can be obtained using the physical condition $p_r(r = \mathcal{R}) = 0$. From the above conditions, we obtain the constraints on the constants s_1 , s_2 and s_5 . Using the above constraints, we obtain the constants s_1 , s_2 and s_5 as follows:

$$s_1 = -\frac{8 s_3 M^2 - 5 s_3 \mathcal{R} M - 4 s_4 \pi \mathcal{R}^4}{\mathcal{R}^2 s_3 (\mathcal{R} - 2 M)^2}, \quad s_2 = \frac{-3 s_3 \mathcal{R} M + 4 s_3 M^2 - 4 s_4 \pi \mathcal{R}^4}{\mathcal{R}^4 s_3 (\mathcal{R} - 2 M)^2},$$

$$s_5 = \frac{(\mathcal{R} - 2 M)}{\mathcal{R}} e^{\frac{(36 M^2 - 21 \mathcal{R} M) s_3^2 - 12 \ln\left(\frac{\mathcal{R}}{\mathcal{R} - 2 M}\right) (\mathcal{R} - 2 M)^2 s_3^2 + (36 M^2 - 64 M^2 \mathcal{R}^2 s_4 \pi + 120 M s_4 \pi \mathcal{R}^3 - 21 \mathcal{R} M - 60 s_4 \pi \mathcal{R}^4) s_3 - 32 \mathcal{R}^6 s_4^2 \pi^2 - 12 s_4 \pi \mathcal{R}^4}{12(\mathcal{R} - 2 M)^2 s_3}}}. \quad (23)$$

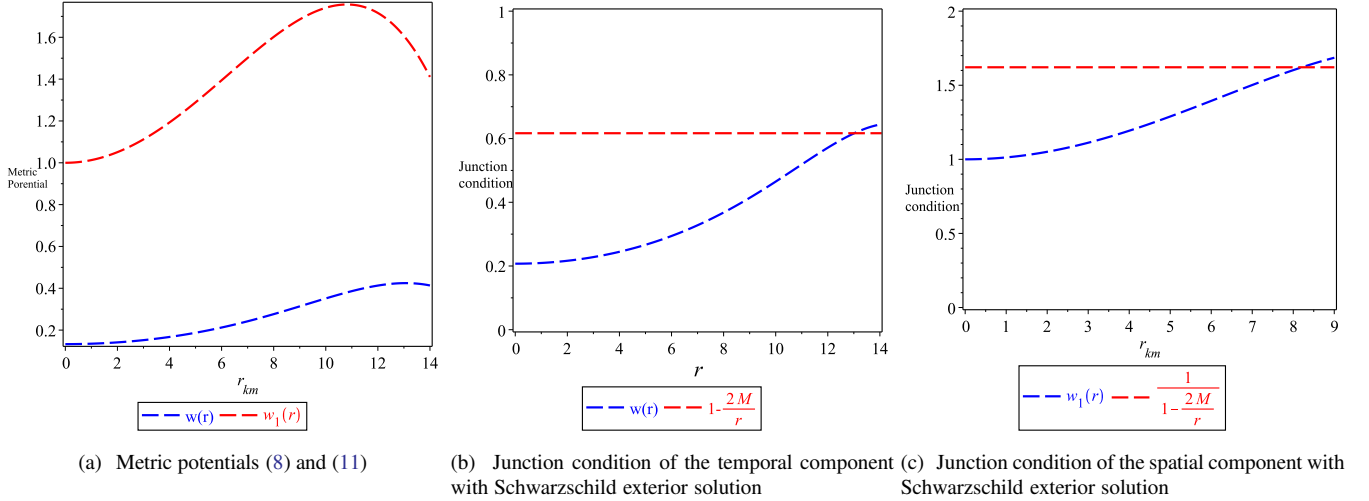


Figure 1. [

figtopcap]Schematic plots: (a) the metric potentials (8) and (11); (b) the junction condition at the surface boundary of star between the metric potential $w(r)$ and the temporal potential of Schwarzschild; (c) the junction condition at the surface boundary of star between the metric potential $w_1(r)$ and the spatial potential of Schwarzschild.

The constant s_4 , is determined from the fact that $p_r(r = \mathcal{R}) = 0 \Rightarrow s_4 = -s_3\rho(r = \mathcal{R})$ and the constant s_3 remains arbitrary so that its value will be adjusted with the real compact star.

6. MATCHING THE MODEL WITH THE REALISTIC COMPACT STARS

Let us now consider the previous physical conditions of the model derived to test it using the masses and radii of the observed pulsars. To support our model, the pulsar 4U 1820-30 whose estimated mass and radius are $M = 1.46 \pm 0.21 M_\odot$ and $\mathcal{R} = 11.1 \pm 1.8$ km, respectively, will be studied (Gangopadhyay et al. 2013; Das et al. 2021; Roupas & Nashed 2020). The maximal values $M = 1.67 M_\odot$ and $\mathcal{R} = 12.9$ km can be used as the input parameters. The boundary conditions are adopted to determine the constants $s_1 = 0.01294823993$, $s_2 = -0.00005537504986$, and $s_5 = 0.5917241379 e^{-0.7529881502 - 1.480957408 s_3}$.

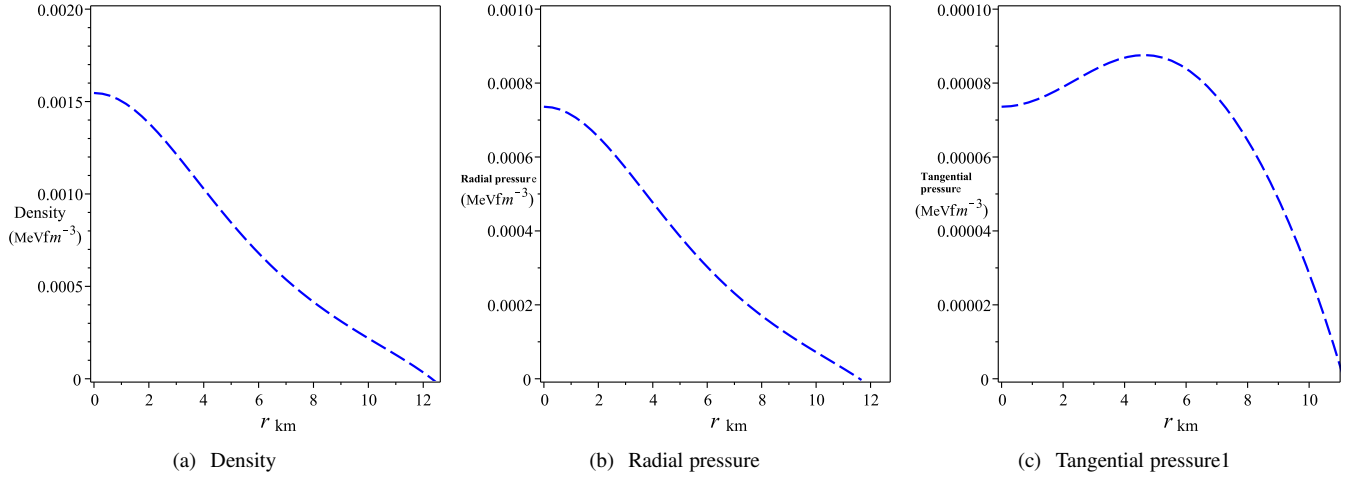
Adopting these constants, the physical quantities can be plotted. The regular behavior of these can be assumed as being a first requirement to fit a realistic star model. Figure 1 (a) represents the behavior of metric potentials for 4U 1820-30 as well as the junction conditions. As Figure 1 shows, the metric potentials assume the values $w(0) = 0.1328969066$ and $w_1(0) = 1$ for $r = 0$ and $s_3 = 0.5$. This means that they are both finite and positive at the center.

The metric potentials of solution (12) are plotted in Figure 1 (a); Figure 1 (b) represents the junction condition of the temporal metric potential (11) and the temporal metric potential of the Schwarzschild solution. Figure 1 (c) represents the junction condition of the spatial metric potential (8) and the spatial metric potential of the Schwarzschild solution. Figure 2 shows that density, radial and tangential pressures are positive as required for realistic stellar configuration. Moreover, as Figure 2 (a) shows, the density is high at the center, $\rho(r = 0) = 0.001546366234$ and decreases with the distance from it. Figure 2 (b) shows that the radial pressure tends to be zero at the boundary; which is relevant for a realistic model. Figure 2 (c) shows that the tangential pressure has a positive value and that it has a high value at the center, decrease away from the center.

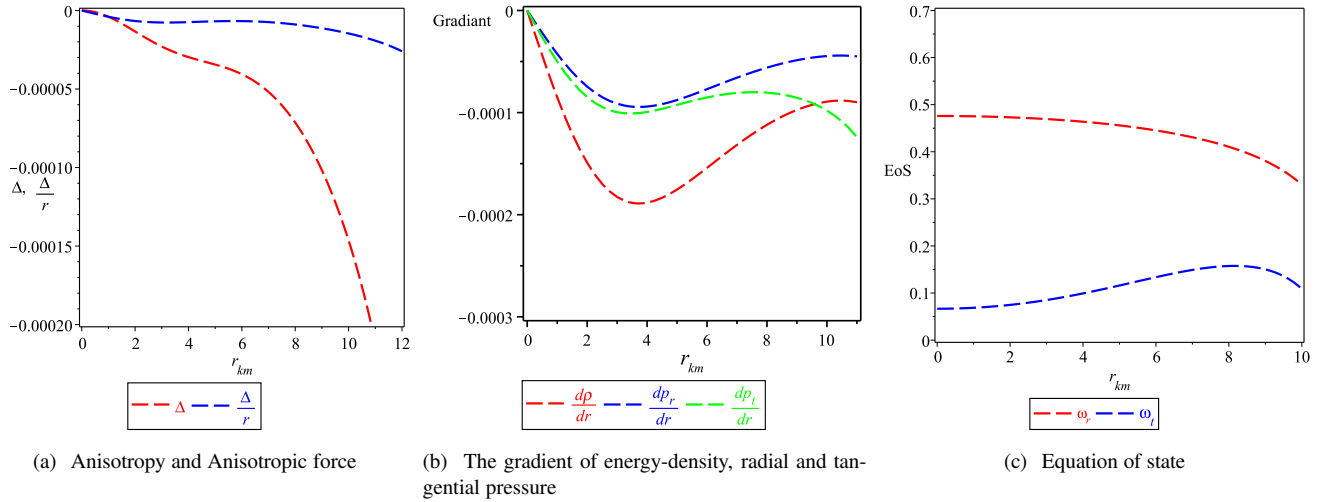
Figure 3 (a) shows that the anisotropy, $\Delta(r) = p_t - p_r$ and the anisotropic force. As Figure 3 (a) shows, the anisotropy vanishes at the center and decreases at the surface of the star. In particular, Fig. 3 (a) shows that the anisotropic force $\frac{\Delta}{r}$ is negative. This means that it possesses an inward gravitational since $p_r - p_t > 0$. Figure 3 (b) shows that the gradients of density, radial and tangential pressures are negative confirming the decreasing of density, radial and transverse pressures through the stellar configuration. Also Fig. 3 (c) shows that the radial and tangential EoSs are positive within the star configuration.

Figures 4 (a), 4 (b), 4 (c) and 4 (d) show the positive values of the WEC, NEC, SEC and DEC. Therefore, all the energy conditions are satisfied throughout the stellar configuration as required for a physically meaningful stellar model.

Figure 5 (a) represents the velocity of the sound, radial and transverse, speeds; this should be less than the speed of the light, i.e., $\frac{dp_r}{dp} < 1$ and $\frac{dp_t}{dp} < 1$. This condition is known as the causality condition. The mass function given by Eq. (14) is plotted in Fig. 5(b), showing that it is a monotonically increasing function of the radial coordinate and $M(r = 0) = 0$. Furthermore, Figure 5(b) shows the behavior of the compactness parameter of star which is increasing. The radial variation of the surface redshift is

**Figure 2.** [

figtopcap]Plot of the radial coordinate r in km vs. the density, radial and tangential pressures of (12) using the constants constrained from 4U 1820-30.

**Figure 3.** [

figtopcap]Schematic plots: (a) of the radial coordinate r in km vs. the anisotropy and anisotropic force of solution (12) using the constants constrained from 4U 1820-30; (b) the radial coordinate r in km vs. the gradient of density, radial and tangential pressures of solution (12) using the constants constrained from 4U 1820-30; (c) the radial and tangential equation of states using the constants constrained from 4U 1820-30.

plotted in Figure 5(c). Böhmer and Harko (Böhmer & Harko 2006) constrained the surface red-shift to be $Z \leq 5$. The surface redshift of this model is calculated according to 4U1820 – 30 and is found to be ≈ 0.008 .

7. STABILITY OF THE MODEL

In this section we are going to discuss the stability issue using two different techniques; the TOV equations and the adiabatic index.

7.1. Equilibrium analysis through TOV equation

In this subsection, we are going to discuss the stability of any stellar model. For this goal, we assume hydrostatic equilibrium through the TOV equation. Using the TOV equation (Tolman 1939; Oppenheimer & Volkoff 1939) as that presented in (Ponce de Leon 1993), we obtain the following form:

$$\frac{2[p_t - p_r]}{r} - \frac{M_g(r)[\rho(r) + p_r] \sqrt{w}}{r \sqrt{w_1}} - \frac{dp_r}{r} = 0, \quad (24)$$

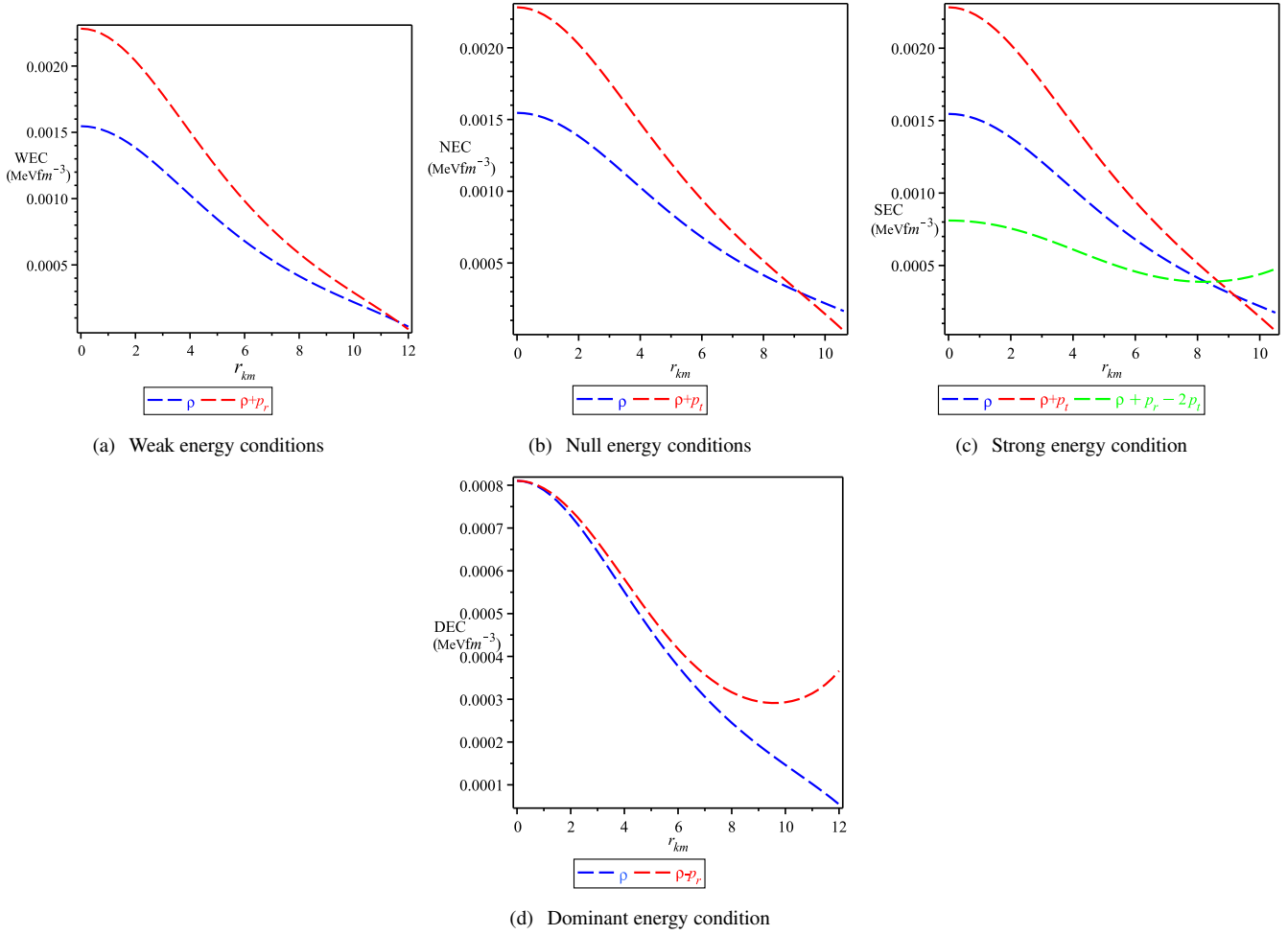


Figure 4. [

figtopcap]Schematic plots: (a) the weak, (b) null, (c) strong and (d) dominant energy conditions of solution (12) using the constants constrained from 4U 1820-30.

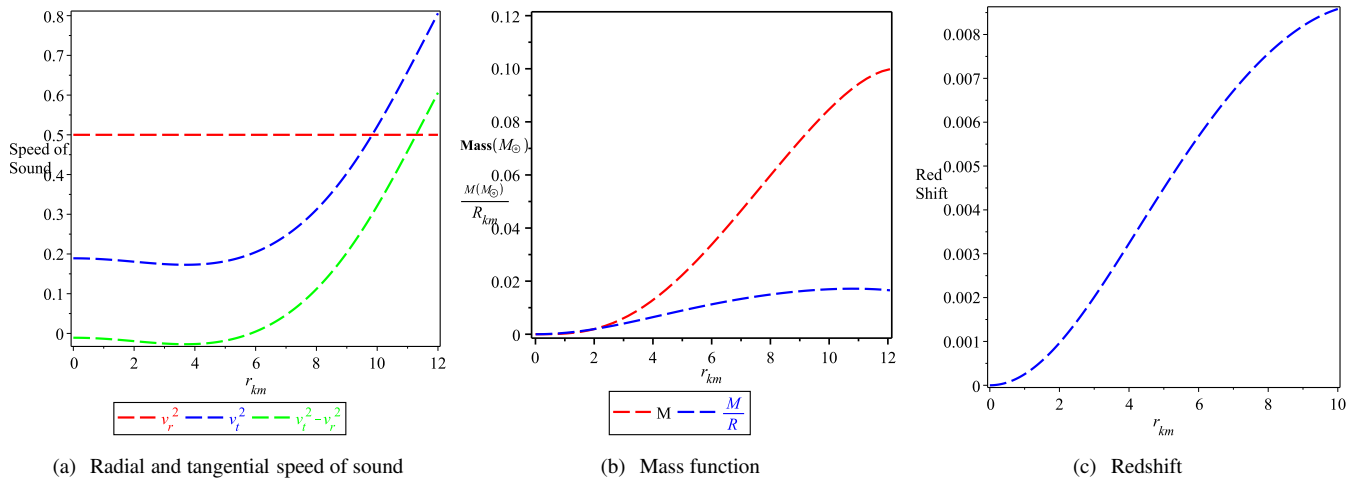


Figure 5. [

figtopcap]Schematic plots: (a) of the radial coordinate r in km vs, the radial, tangential speeds of solution (12) and the difference between the radial and tangential speeds of sound; (b) the mass and compactness vs the radial coordinate r in km (c) the surface red-shift vs the radius r using the constants constrained from 4U 1820-30.

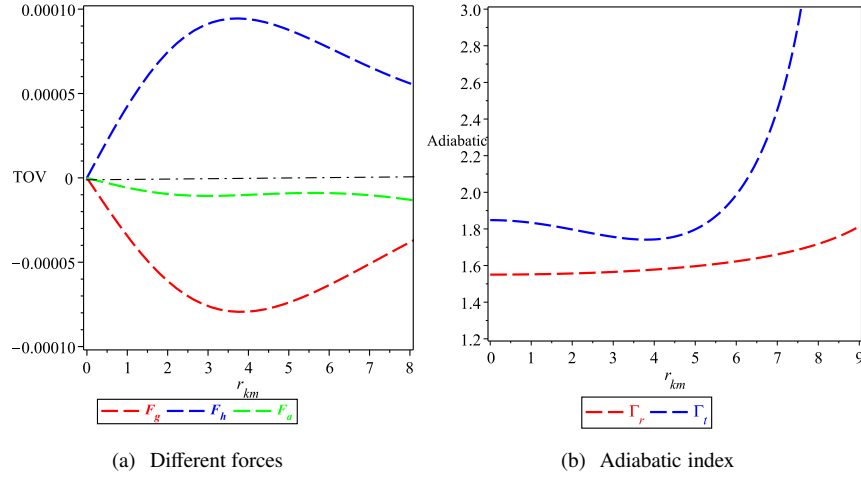


Figure 6. [

figtopcap]Schematic plots: (a) the gravitational, the anisotropic and the hydrostatic forces vs. the radius r ; (b) the adiabatic index vs. the radius r using the constants constrained from 4U 1820-30.

with $M_g(r)$ being the gravitational mass at radius r , as defined by the Tolman-Whittaker mass formula which gives:

$$M_g(r) = 4\pi \int_0^r \left(T_t^t - T_r^r - T_\theta^\theta - T_\phi^\phi \right) r^2 \sqrt{ww_1} dr = \frac{rw' \sqrt{w_1}}{2w}, \quad (25)$$

Inserting Eq. (25) into (24), we obtain:

$$\frac{2(p_t - p_r)}{r} - \frac{dp_r}{dr} - \frac{w'[\rho + p_r]}{2\sqrt{w}} = F_g + F_a + F_h = 0, \quad (26)$$

where $F_g = -\frac{w'[\rho + p_r]}{2\sqrt{w}}$, $F_a = \frac{2(p_t - p_r)}{r}$, and $F_h = -\frac{dp_r}{dr}$ are the gravitational, anisotropic and hydrostatic forces, respectively. The behavior of the TOV equation for model (12) is shown in Figure 6 in which the three different forces are plotted. This shows that hydrostatic force is positive and is dominated by the gravitational and anisotropic forces, which are negative to maintain the system in static equilibrium.

7.2. Adiabatic index

The stable equilibrium configuration of a spherically symmetric system can be studied using the adiabatic index, which is a basic ingredient of the stability criterion. Let us consider an adiabatic perturbation, the adiabatic index Γ , is defined as (Chandrasekhar 1964; Nashed 2002; Merafina & Ruffini 1989; Chan et al. 1993):

$$\Gamma = \left(\frac{\rho + p}{p} \right) \left(\frac{dp}{d\rho} \right). \quad (27)$$

A Newtonian isotropic sphere is in stable equilibrium if the adiabatic index $\Gamma > \frac{4}{3}$ as reported in Heintzmann and Hillebrandt (Heintzmann & Hillebrandt 1975). For $\Gamma = \frac{4}{3}$, the isotropic sphere is in neutral equilibrium. Based on some works carried out by Chan et al. (Chan et al. 1993), the following condition is required for the stability of a relativistic anisotropic sphere $\Gamma > \gamma$ where:

$$\gamma = \frac{4}{3} - \left\{ \frac{4(p_r - p_t)}{3|p_r'|} \right\}_{max}. \quad (28)$$

Using Eq. (28), we obtain:

$$\Gamma = \frac{4}{3} - \frac{2}{3} \left[(c_2 r^2 + 1)^2 (4k_1^2 k^8 + 6k^4 - 8r^2 k^2 + 3r^4) \right] \times \left[2(c_2 r^2 + 1)^2 k^8 k_1^2 + 16k^6 c_2 - 18c_2^2 r^4 k^4 - 36k^4 c_2 r^2 + 6k^4 + 16c_2 r^4 k^2 - 16k^2 r^2 + 16c_2^2 r^6 k^2 + 2c_2 r^6 + 9r^4 - 3c_2^2 r^8 + 4c_2^2 k^8 \right]^{-1}. \quad (29)$$

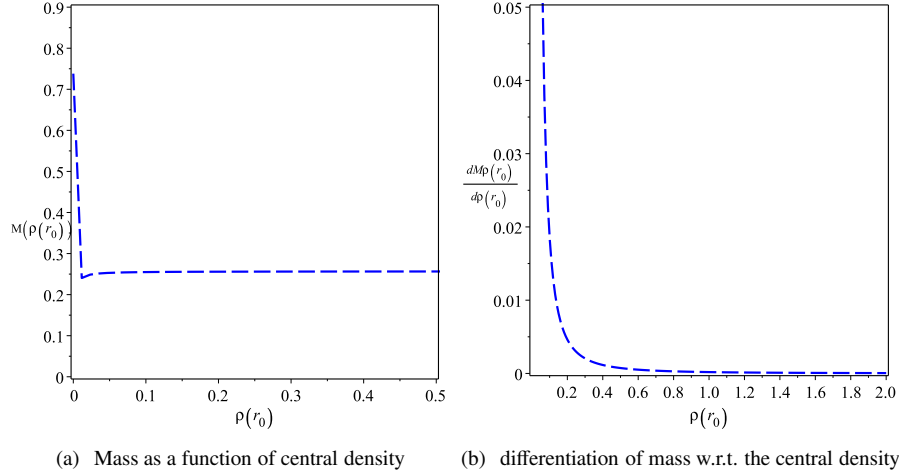


Figure 7. [

figtopcap]Schematic plots: (a) the gravitational mass as a function of the central density; (b) the differentiation of gravitational mass w.r.t. the central density using the constrained from 4U 1820-30.

From Eq. (27), we obtain the adiabatic index of solution (12) in the form:

$$\begin{aligned}
 \Gamma_r = s_3 & \left(8 s_4 \pi r^8 s_2^2 + 16 r^6 s_4 \pi s_1 s_2 + r^6 s_3 s_2^2 + 8 r^4 s_4 \pi s_1^2 + 2 r^4 s_2 s_3 s_1 + 16 s_4 \pi r^4 s_2 + r^2 s_3 s_1^2 + 16 s_4 \pi r^2 s_1 \right. \\
 & \left. + 5 s_3 r^2 s_2 + 3 s_3 s_1 + 8 s_4 \pi + s_2^2 r^6 + 2 s_1 r^4 s_2 + 5 s_2 r^2 + r^2 s_1^2 + 3 s_1 \right) \times \left\{ 8 s_4 \pi r^8 s_2^2 + 16 r^6 s_4 \pi s_1 s_2 + r^6 s_3 s_2^2 \right. \\
 & \left. + 8 r^4 s_4 \pi s_1^2 + 2 r^4 s_2 s_3 s_1 + 16 s_4 \pi r^4 s_2 + r^2 s_3 s_1^2 + 16 s_4 \pi r^2 s_1 + 5 s_3 r^2 s_2 + 3 s_3 s_1 + 8 s_4 \pi \right\}^{-1}. \quad (30)
 \end{aligned}$$

In Fig. 6(b) Γ_r and Γ_t are reported. As can be seen from these plots, the value of Γ_t is greater than that of Γ_r throughout the stellar interior, and hence, the stability condition is fulfilled.

7.3. Stability in the static state

For stable compact stars in terms of the mass-central mass–radius, and relations for the energy density, Harrison, Zeldovich, and Novikov (Harrison et al. 1965; Zeldovich & Novikov 1971) claimed that the gradient of the central density, with respect to the mass, must be positive, i.e., $\frac{\partial M}{\partial \rho_{r_0}} > 0$. If this condition is satisfied, then we have stable configurations. To be more specific, the stable stable or unstable region is satisfied for constant mass i.e. $\frac{\partial M}{\partial \rho_{r_0}} = 0$ (Singh et al. 2019). Let us apply this procedure to our solution (12). For solution (12), the central density has the form:

$$\begin{aligned}
 \rho_{r_0} = \frac{3s_1}{8\pi} & \Rightarrow s_1 = \frac{8\pi\rho_{r_0}}{3}, \\
 M(\rho_{r_0}) & = \frac{R^3(8\pi\rho_{r_0} + 3s_2R^2)}{16\pi(3 + 8\pi R^2\rho_{r_0} + 3s_2R^4)}. \quad (31)
 \end{aligned}$$

With Eq. (31) we have:

$$\frac{\partial M}{\partial \rho_{r_0}} = \frac{3R^3}{2(3 + 8\pi R^2\rho_{r_0} + 3s_2R^4)^2}. \quad (32)$$

From Eq. (32), the solution (12) has a stable configuration since $\frac{\partial M}{\partial \rho_{r_0}} > 0$ (Singh et al. 2019). The behaviors of (31) and (32) are shown in Fig. 7. It follows from these figures that the mass and the gradient-of-mass decrease as the energy density become larger. The above discussion of solution (12) shows that we have a good model.

In addition to 4U 1820-30, a similar analysis can be developed for other pulsars. In Tables I and II, we report the results for other observed systems.

Table 1. Values of model parameters (Özel et al. 2016)

Pulsar	Mass (M_{\odot})	Radius (km)	s_1	s_2	s_3	s_4	s_5
4U 1724-207	$1.81^{+0.25}_{-0.37}$	$12.2^{+1.4}_{-1.4}$	≈ 0.013	$\approx -0.45 \times 10^{-4}$	0.5	$\approx -0.18 \times 10^{-12}$	≈ 0.10
4U 1820-30	$1.46^{+0.21}_{-0.21}$	$11.1^{+1.8}_{-1.8}$	≈ 0.011	$\approx -0.41 \times 10^{-4}$	0.5	$\approx -0.76 \times 10^{-13}$	≈ 0.12
SAX J1748.9-2021	$1.81^{+0.25}_{-0.37}$	$11.7^{+1.7}_{-1.7}$	≈ 0.014	$\approx -0.5 \times 10^{-4}$	0.5	$\approx -0.59 \times 10^{-13}$	≈ 0.11
EXO 1745-268	$1.65^{+0.21}_{-0.31}$	$10.5^{+1.6}_{-1.6}$	≈ 0.017	$\approx -0.75 \times 10^{-4}$	0.5	$\approx -0.59 \times 10^{-13}$	≈ 0.14
4U 1608-52	$1.57^{+0.30}_{-0.29}$	$9.8^{+1.8}_{-1.8}$	≈ 0.02	$\approx -0.99 \times 10^{-4}$	0.5	$\approx -0.33 \times 10^{-12}$	≈ 0.17
KS 1731-260	$1.61^{+0.35}_{-0.37}$	$10.0^{+2.2}_{-2.2}$	≈ 0.018	$\approx -0.8 \times 10^{-4}$	0.5	$\approx -0.27 \times 10^{-12}$	≈ 0.13

Table 2. Values of physical quantities

Pulsar	$\rho _0$	$\rho _R$	$\frac{dp_r}{d\rho} _0$	$\frac{dp_r}{d\rho} _R$	$\frac{dp_t}{d\rho} _0$	$\frac{dp_t}{d\rho} _R$	$(\rho - p_r - 2p_t) _0$	$(\rho - p_r - 2p_t) _R$	$z _R$
4U 1724-207	0.15×10^{-2}	$.36 \times 10^{-12}$.5	.5	.56	2.13	$.76 \times 10^{-3}$	$.63 \times 10^{-3}$.009
4U 1820-30	0.13×10^{-2}	0	.5	.5	.59	1.87	$.63 \times 10^{-4}$	$.6 \times 10^{-4}$.0077
SAX J1748.9-2021	0.16×10^{-2}	1.18×10^{-13}	.5	.5	.56	2.16	$.81 \times 10^{-3}$	$.66 \times 10^{-3}$.0092
EXO 1745-268	0.20×10^{-2}	1.33×10^{-8}	.5	.5	.56	2.16	$.1 \times 10^{-2}$	$.8 \times 10^{-3}$.0092
4U 1608-52	$.24 \times 10^{-2}$	6.53×10^{-14}	.5	.5	.55	2.26	$.12 \times 10^{-2}$	$.92 \times 10^{-3}$.0096
KS 1731-260	0.22×10^{-2}	2.2×10^{-13}	.5	.5	.55	2.25	$.11 \times 10^{-2}$	$.83 \times 10^{-3}$.0096

8. DISCUSSION AND CONCLUSIONS

In this research, we studied anisotropic spherically symmetric spacetime in the frame of MGT. We obtained a system of three differential equations in six unknowns. To put this system in a closed form, we used the formula of the radial component of the metric potential given by Tolman (Tolman 1939), a linear form of the radial EoS, and the constraint given by the mimetic field and the metric potential g_{rr} given by Eq. (2). The solution of this system involves five constants, three of them are fixed using the junction condition, matching the interior solution with the Schwarzschild exterior, as well as the vanishing of the radial pressure at the boundary. The fourth constant is determined from the radial EoS, leaving the fifth constant to be determined from the study of a real compact star. The main features of this study can be summarized as follows:

★ To demonstrate that our solution is compatible with a real compact star, we used the stellar 4U1820 – 30, which has mass $1.46^{+0.21}_{-0.21} M_{\odot}$, and radius $11.1^{+1.8}_{-1.8}$ km (Roupas & Nashed 2020; Das et al. 2021). The use of the mass and the radius fixed the two constants $s_1 = 0.01049285312$ and $s_2 = -.4062000611 \times 10^{-4}$. Furthermore, the use of the vanishing of the radial pressure on the boundary yields $s_5 = .1195529130$. Finally, using the linear radial EoS through the assumption of $s_3 = 0.5$ we obtained the constant $s_4 = .7572649088 \times 10^{-13}$.

★ As shown in Figure 1, the metric potentials have no singularity either at the center of the star or at the boundary. Furthermore, in Figure 1 we show how the junction condition is made between the interior and exterior Schwarzschild solution.

★ Figure 2, shows that the density, radial, and tangential pressures are positive and decrease toward the center of the star.

★ Figure 3, shows that the anisotropic force has a negative sign, meaning that it is attractive since $p_t - p_r < 0$. Also, figure 3, 3 shows that the gradient of the density, radial, and tangential pressures are negative; this is a necessary condition for any real star configuration. Finally, Figure 3 shows that the radial and tangential EoS's are not constant.

★ The importance of energy conditions in the frame of modified gravitational theories were discussed in detail in (Capozziello et al. 2015, 2014). In the present study, we tested the impact of extra force which comes from the mimetic field and get the matter content more realistic, as in the case of all these stars, the energy conditions, i.e., NEC, WEC, DEC, SEC were all well satisfied which support that the matter destination is normal matter (not any kind of exotic matter). In figure 4, 4 shows that our model satisfies all the energy conditions. Furthermore, Figure 5 shows that the radial and tangential speeds are

≤ 1 , as required for any realistic star. Also in figure 5 the mass and compactness of our model are positive, and the red-shift is less than five i.e., $Z < 5$.

★ Figure 6, shows that the resulting model is stable because its adiabatic index is greater than $4/3$.

★ Finally, we extended our study to other stars, as shown in Tables I and II, which confirms that our model is verified for these compact stars.

★ It is interesting to analyze the solutions presented in this study in the frame of more compact objects like neutron stars, to make contact with events like the *GW190814*. These solutions have been discussed in details in (Astashenok et al. 2021) in the frame of $f(R)$ gravitational theory. In our case, we must be more careful because our approach applies to inhomogeneous solutions. However, pulsars with spin less than $3ms$ or even the product of the merging of two neutron stars if it is a neutron star, can initially be quite inhomogeneous, thus during the ring-down, our solution could be relevant. We hope to discuss this topic in future work since such a study would require the implementation of a numerical recipe appropriately tailored to our solutions.

Appendix A

The form of tangential pressure and anisotropic force

$$\begin{aligned}
p_t(r) = & \frac{1}{32\pi (1 + s_1 r^2 + s_2 r^4)^3} \left[144 s_4 \pi r^4 s_2 + 128 s_4 \pi r^2 s_1 + 208 s_4 \pi r^8 s_2^2 + 64 s_4^2 \pi^2 r^{18} s_2^4 + 176 r^4 s_4 \pi s_1^2 + 26 r^4 s_3 s_1 s_2 \right. \\
& + 384 r^6 s_4 \pi s_1 s_2 + 40 s_3 r^2 s_2 + 8 s_1 r^4 s_2 + 12 s_3 s_1 + 32 s_4 \pi + 5 s_2^2 r^6 + 3 r^2 s_1^2 + 6 r^6 s_3 s_2^2 + 8 r^2 s_3 s_1^2 + 64 s_2^3 r^{14} s_4 \pi s_1 s_3 \\
& + 96 s_2^2 r^{12} s_4 \pi s_1^2 s_3 + 64 r^{10} s_4 \pi s_2 s_1^3 s_3 + 304 r^{10} \pi s_4 s_2^2 s_1 s_3 + 272 r^8 s_4 \pi s_2 s_1^2 s_3 + 288 r^6 s_4 \pi s_1 s_2 s_3 + 2 s_2^4 r^{14} s_3 \\
& + s_2^4 r^{14} s_3^2 + 2 r^6 s_1^4 s_3 + r^6 s_1^4 s_3^2 + 14 r^6 s_2 s_1^2 + 4 r^8 s_1^3 s_2 + 16 r^8 s_2^2 s_1 + 10 r^4 s_1^3 s_3 + 6 r^4 s_1^3 s_3^2 + 64 r^2 \pi^2 s_4^2 + 9 r^2 s_1^2 s_3^2 \\
& + 25 r^6 s_2^2 s_3^2 + 6 r^{10} s_2^2 s_1^2 + 10 r^{10} s_2^3 s_3^2 + 16 r^{10} s_2^3 s_3 + 4 s_2^3 r^{12} s_1 + 256 \pi^2 s_4^2 s_2^3 r^{16} s_1 + 16 \pi s_4 s_2^4 r^{16} s_3 \\
& + 384 s_2^2 r^{14} s_4^2 \pi^2 s_1^2 + 64 s_2^3 r^{14} s_4 \pi s_1 + 256 s_2 r^{12} s_4^2 \pi^2 s_1^3 + 96 s_2^2 r^{12} s_4 \pi s_1^2 + 768 s_2^2 r^{12} s_1 \pi^2 s_4^2 + 112 s_2^3 r^{12} s_4 \pi s_3 \\
& + 64 r^{10} s_4 \pi s_2 s_1^3 + 768 r^{10} s_2 s_1^2 \pi^2 s_4^2 + 320 r^{10} \pi s_4 s_2^2 s_1 + 16 r^8 s_4 \pi s_1^4 s_3 + 304 r^8 s_4 \pi s_2 s_1^2 + 768 r^8 s_2 s_1 \pi^2 s_4^2 \\
& + 176 r^8 s_4 \pi s_2^2 s_3 + 80 r^6 \pi s_4 s_1^3 s_3 + 112 r^4 s_4 \pi s_1^2 s_3 + 80 r^4 s_4 \pi s_2 s_3 + 48 r^2 s_4 \pi s_1 s_3 + 16 \pi s_4 s_2^4 r^{16} + 256 s_2^3 r^{14} s_4^2 \pi^2 \\
& + 8 s_2^3 r^{12} s_1 s_3 + 4 s_2^3 r^{12} s_1 s_3^2 + 112 s_2^3 r^{12} s_4 \pi + 64 r^{10} s_4^2 \pi^2 s_1^4 + 12 r^{10} s_2^2 s_1^2 s_3 + 6 r^{10} s_2^2 s_1^2 s_3^2 + 384 r^{10} s_4^2 \pi^2 s_2^2 \\
& + 16 r^8 s_4 \pi s_1^4 + 8 r^8 s_1^3 s_3 s_2 + 4 r^8 s_1^3 s_2 s_3^2 + 256 r^8 s_4^2 \pi^2 s_1^3 + 42 r^8 s_2^2 s_1 s_3 + 26 r^8 s_2^2 s_1 s_3^2 + 96 r^6 \pi s_4 s_1^3 + 36 r^6 s_1^2 s_3 s_2 \\
& \left. + 22 r^6 s_1^2 s_2 s_3^2 + 384 r^6 s_4^2 \pi^2 s_1^2 + 256 r^6 s_4^2 \pi^2 s_2 + 30 r^4 s_1 s_2 s_3^2 + 256 r^4 s_1 \pi^2 s_4^2 + s_2^4 r^{14} + 6 r^{10} s_2^3 + r^6 s_1^4 + 4 r^4 s_1^3 \right], \\
\Delta = & \frac{r^2}{32\pi (1 + s_1 r^2 + s_2 r^4)^3} \left[3 s_1^2 + 16 r^6 s_4 \pi s_1^4 + 8 r^6 s_1^3 s_3 s_2 + 4 r^6 s_1^3 s_2 s_3^2 + 256 r^6 s_4^2 \pi^2 s_1^3 + 26 r^6 s_1 s_2^2 s_3^2 \right. \\
& + 30 r^6 s_1 s_2^2 s_3 + 64 r^4 s_4 \pi s_1^3 + 22 r^4 s_1^2 s_2 s_3^2 + 24 r^4 s_1^2 s_3 s_2 + 384 r^4 s_4^2 \pi^2 s_1^2 + 256 r^4 s_4^2 \pi^2 s_2 + 80 r^2 s_4 \pi s_1^2 + 30 r^2 s_1 s_2 s_3^2 \\
& - 14 r^2 s_2 s_3 s_1 + 256 r^2 s_1 s_4^2 \pi^2 + 48 r^2 s_4 \pi s_2 + 64 s_4^2 \pi^2 r^{16} s_2^4 + 16 s_4 \pi s_2^4 r^{14} + 256 s_2^3 r^{12} s_4^2 \pi^2 + 8 s_2^3 r^{10} s_1 s_3 \\
& + 4 s_2^3 r^{10} s_1 s_3^2 + 80 s_2^3 r^{10} s_4 \pi + 64 r^8 s_4^2 \pi^2 s_1^4 + 12 r^8 s_2^2 s_1^2 s_3 + 6 r^8 s_2^2 s_1^2 s_3^2 + 384 r^8 s_4^2 \pi^2 s_2^2 + 112 s_4 \pi r^6 s_2^2 \\
& + 48 s_4 \pi s_1 s_3 + 5 s_2^2 r^4 + 8 s_1 r^2 s_2 + 4 r^6 s_2 s_1^3 + 16 r^6 s_2^2 s_1 + 2 r^4 s_1^4 s_3 + r^4 s_1^4 s_3^2 + 14 r^4 s_2 s_1^2 - 18 r^4 s_3 s_2^2 + 25 r^4 s_2^2 s_3^2 \\
& + 6 r^2 s_1^3 s_3 + 6 r^2 s_1^3 s_3^2 + s_2^4 r^{12} s_3^2 + 4 s_2^3 r^{10} s_1 + 2 s_2^4 r^{12} s_3 + 12 r^8 s_2^3 s_3 + 10 r^8 s_2^3 s_3^2 + 6 r^8 s_2^2 s_1^2 + 9 s_1^2 s_3^2 + r^4 s_1^4 \\
& + 4 r^2 s_1^3 + s_2^4 r^{12} + 6 r^8 s_2^3 + 64 s_4^2 \pi^2 + 20 s_3 s_2 - 8 s_3 s_1^2 + 32 s_4 \pi s_1 + 224 r^8 s_4 \pi s_2^2 s_1 + 16 r^6 s_4 \pi s_1^4 s_3 + 208 r^6 s_4 \pi s_2 s_1^2 \\
& + 768 r^6 s_1 s_2 s_4^2 \pi^2 + 176 r^6 s_4 \pi s_2^2 s_3 + 80 r^4 s_4 \pi s_1^3 s_3 + 192 r^4 s_4 \pi s_1 s_2 + 112 r^2 s_4 \pi s_1^2 s_3 + 80 r^2 s_4 \pi s_2 s_3 \\
& + 256 s_4^2 \pi^2 s_2^3 r^{14} s_1 + 16 s_4 \pi s_2^4 r^{14} s_3 + 384 s_2^2 r^{12} s_4^2 \pi^2 s_1^2 + 64 s_2^3 r^{12} s_4 \pi s_1 + 256 s_2 r^{10} s_4^2 \pi^2 s_1^3 + 96 s_2^2 r^{10} s_4 \pi s_1^2 \\
& + 768 s_2^2 r^{10} s_1 s_4^2 \pi^2 + 112 s_2^3 r^{10} s_4 \pi s_3 + 64 r^8 s_4 \pi s_2 s_1^3 + 768 r^8 s_2 s_1^2 s_4^2 \pi^2 + 64 s_2^3 r^{12} s_4 \pi s_1 s_3 + 96 s_2^2 r^{10} s_4 \pi s_1^2 s_3 \\
& \left. + 64 r^8 s_4 \pi s_2 s_1^3 s_3 + 304 r^8 s_4 \pi s_2^2 s_1 s_3 + 272 r^6 s_4 \pi s_2 s_1^2 s_3 + 288 r^4 s_4 \pi s_1 s_2 s_3 \right]. \quad (\mathbf{A})
\end{aligned}$$

Appendix B

The gradient of the tangential pressure

$$\begin{aligned}
 p'_t = & \frac{r}{16\pi (1 + s_1 r^2 + s_2 r^4)^4} \left[-28 s_3 s_1^2 + 40 s_3 s_2 + 64 s_4^2 \pi^2 + 9 s_1^2 s_3^2 + 15 s_2^2 r^4 + s_2^4 r^{12} + 15 r^8 s_2^3 - r^4 s_1^4 + 2 r^2 s_1^3 \right. \\
 & + 3072 s_4^2 \pi^2 s_2^3 r^{14} s_1 + 128 s_4 \pi s_2^4 r^{14} s_3 + 4224 s_2^2 r^{12} s_4^2 \pi^2 s_1^2 + 464 s_2^3 r^{12} s_4 \pi s_1 + 2560 s_2 r^{10} s_4^2 \pi^2 s_1^3 + 608 s_2^2 r^{10} s_4 \pi s_1^2 \\
 & + 3840 s_2^2 r^{10} s_1 s_4^2 \pi^2 + 320 s_2^3 r^{10} s_4 \pi s_3 + 336 r^8 s_4 \pi s_2 s_1^3 + 3456 r^8 s_2 s_1^2 s_4^2 \pi^2 + 656 r^8 s_4 \pi s_2^2 s_1 + 64 r^6 s_4 \pi s_1^4 s_3 \\
 & + 512 r^6 s_4 \pi s_2 s_1^2 + 2048 r^6 s_2 s_1 s_4^2 \pi^2 + 384 r^6 s_4 \pi s_2^2 s_3 + 128 r^4 s_4 \pi s_1^3 s_3 + 368 r^4 s_4 \pi s_1 s_2 + 128 r^2 s_4 \pi s_1^2 s_3 \\
 & + 160 r^2 s_4 \pi s_2 s_3 + 1664 s_4^2 \pi^2 s_2^3 r^{16} s_1^2 + 896 s_4^2 \pi^2 s_2^4 r^{18} s_1 + 32 s_4 \pi s_2^5 r^{18} s_3 + 1536 s_2^2 r^{14} s_4^2 \pi^2 s_1^3 + 256 s_2^3 r^{14} s_4 \pi s_1^2 \\
 & + 144 s_2^4 r^{16} s_4 \pi s_1 + 704 s_2 r^{12} s_4^2 \pi^2 s_1^4 + 224 s_2^2 r^{12} s_4 \pi s_1^3 + 96 r^{10} s_4 \pi s_2 s_1^4 + 16 r^8 s_4 \pi s_1^5 s_3 + 48 s_4 \pi s_1 s_3 + 96 s_4 \pi r^2 s_2 \\
 & + 256 s_4 \pi r^6 s_2^2 + 832 s_4^2 \pi^2 r^{16} s_2^4 + 128 s_4 \pi s_2^4 r^{14} + 1408 s_2^3 r^{12} s_4^2 \pi^2 - 4 s_2^3 r^{10} s_1 s_3 - 8 s_2^3 r^{10} s_1 s_3^2 + 256 s_2^3 r^{10} s_4 \pi \\
 & + 576 r^8 s_4^2 \pi^2 s_1^4 - 6 r^8 s_2^2 s_1^2 s_3 - 10 r^8 s_2^2 s_1^2 s_3^2 + 1152 r^8 s_4^2 \pi^2 s_2^2 + 64 r^6 s_4 \pi s_1^4 - 8 r^6 s_1^3 s_3 s_2 - 8 r^6 s_1^3 s_2 s_3^2 \\
 & + 576 r^8 s_4^2 \pi^2 s_1^4 + 1024 r^6 s_4^2 \pi^2 s_1^3 - 16 r^6 s_2^2 s_1 s_3^2 + 64 r^6 s_2^2 s_1 s_3 + 112 r^4 s_4 \pi s_1^3 - 9 r^4 s_1^2 s_2 s_3^2 + 42 r^4 s_1^2 s_3 s_2 \\
 & + 896 r^4 s_4^2 \pi^2 s_1^2 + 448 r^4 s_4^2 \pi^2 s_2 + 96 r^2 s_4 \pi s_1^2 + 60 r^2 s_1 s_2 s_3^2 - 100 r^2 s_2 s_3 s_1 + 384 r^2 s_1 s_4^2 \pi^2 + 192 s_4^2 \pi^2 r^{20} s_2^5 \\
 & + 32 s_4 \pi s_2^5 r^{18} + 12 s_2^3 r^{12} s_1^2 s_3 + 8 s_2^4 r^{14} s_1 s_3 + 6 s_2^3 r^{12} s_1^2 s_3^2 + 4 s_2^4 r^{14} s_1 s_3^2 + 128 r^{10} s_4^2 \pi^2 s_1^5 + 8 r^{10} s_2^2 s_1^3 s_3 \\
 & + 4 r^{10} s_2^2 s_1^3 s_3^2 + 16 r^8 s_4 \pi s_1^5 + 2 r^8 s_1^4 s_3 s_2 + r^8 s_1^4 s_2 s_3^2 + 3 s_1^2 + 32 s_4 \pi s_1 + s_2^5 r^{16} + 16 s_1 r^2 s_2 + 32 r^6 s_2^2 s_1 - 4 r^4 s_1^4 s_3 \\
 & - 3 r^4 s_1^4 s_3^2 + 19 r^4 s_2 s_1^2 - 182 r^4 s_3 s_2^2 + 75 r^4 s_2^2 s_3^2 + 4 r^2 s_1^3 s_3 - 6 r^2 s_1^3 s_3^2 - 2 s_2^4 r^{12} s_3 - 3 s_2^4 r^{12} s_3^2 + 4 s_2^3 r^{10} s_1 \\
 & + 4 r^8 s_2^2 s_1^2 - 25 r^8 s_2^3 s_3^2 + 62 r^8 s_2^3 s_3 + 144 s_4 \pi s_2^4 r^{16} s_3 s_1 + 96 r^{10} s_4 \pi s_1^4 s_3 s_2 + 256 s_2^3 r^{14} s_4 \pi s_1^2 s_3 \\
 & + 224 s_2^2 r^{12} s_4 \pi s_1^3 s_3 + 480 s_2^3 r^{12} s_4 \pi s_1 s_3 + 640 s_2^2 r^{10} s_4 \pi s_1^2 s_3 + 352 r^8 s_4 \pi s_2 s_1^3 s_3 + 832 r^8 s_4 \pi s_2^2 s_1 s_3 \\
 & \left. + 640 r^6 s_4 \pi s_2 s_1^2 s_3 + 544 r^4 s_4 \pi s_1 s_2 s_3 + r^8 s_1^4 s_2 + 4 r^{10} s_1^3 s_2^2 + 2 s_2^5 r^{16} s_3 + s_2^5 r^{16} s_3^2 + 6 s_2^3 r^{12} s_1^2 + 4 s_2^4 r^{14} s_1 \right], \tag{B}
 \end{aligned}$$

Appendix C

The tangential sound speed

$$\begin{aligned}
 v_r^2 = & \frac{dp_t}{dp} = - \frac{1}{4 (1 + s_1 r^2 + s_2 r^4) (12 s_2^2 r^4 + 3 r^6 s_2^2 s_1 + r^8 s_2^3 + 13 s_1 r^2 s_2 + 3 r^4 s_2 s_1^2 - 5 s_2 + 5 s_1^2 + r^2 s_1^3)} \\
 \times & \left[-28 s_3 s_1^2 + 40 s_3 s_2 + 64 s_4^2 \pi^2 + 9 s_1^2 s_3^2 + 15 s_2^2 r^4 + s_2^4 r^{12} + 15 r^8 s_2^3 - r^4 s_1^4 + 2 r^2 s_1^3 + 3072 s_4^2 \pi^2 s_2^3 r^{14} s_1 \right. \\
 & + 128 s_4 \pi s_2^4 r^{14} s_3 + 4224 s_2^2 r^{12} s_4^2 \pi^2 s_1^2 + 464 s_2^3 r^{12} s_4 \pi s_1 + 2560 s_2 r^{10} s_4^2 \pi^2 s_1^3 + 608 s_2^2 r^{10} s_4 \pi s_1^2 + 3840 s_2^2 r^{10} s_1 s_4^2 \pi^2 \\
 & + 320 s_2^3 r^{10} s_4 \pi s_3 + 336 r^8 s_4 \pi s_2 s_1^3 + 3456 r^8 s_2 s_1^2 s_4^2 \pi^2 + 656 r^8 s_4 \pi s_2^2 s_1 + 64 r^6 s_4 \pi s_1^4 s_3 + 512 r^6 s_4 \pi s_2 s_1^2 \\
 & + 2048 r^6 s_2 s_1 s_4^2 \pi^2 + 384 r^6 s_4 \pi s_2^2 s_3 + 128 r^4 s_4 \pi s_1^3 s_3 + 368 r^4 s_4 \pi s_1 s_2 + 128 r^2 s_4 \pi s_1^2 s_3 + 160 r^2 s_4 \pi s_2 s_3 \\
 & + 1664 s_4^2 \pi^2 s_2^3 r^{16} s_1^2 + 896 s_4^2 \pi^2 s_2^4 r^{18} s_1 + 32 s_4 \pi s_2^5 r^{18} s_3 + 1536 s_2^2 r^{14} s_4^2 \pi^2 s_1^3 + 256 s_2^3 r^{14} s_4 \pi s_1^2 + 144 s_2^4 r^{16} s_4 \pi s_1 \\
 & + 704 s_2 r^{12} s_4^2 \pi^2 s_1^4 + 224 s_2^2 r^{12} s_4 \pi s_1^3 + 96 r^{10} s_4 \pi s_2 s_1^4 + 16 r^8 s_4 \pi s_1^5 s_3 + 48 s_4 \pi s_1 s_3 + 96 s_4 \pi r^2 s_2 + 256 s_4 \pi r^6 s_2^2 \\
 & + 832 s_4^2 \pi^2 r^{16} s_2^4 + 128 s_4 \pi s_2^4 r^{14} + 1408 s_2^3 r^{12} s_4^2 \pi^2 - 4 s_2^3 r^{10} s_1 s_3 - 8 s_2^3 r^{10} s_1 s_3^2 + 256 s_2^3 r^{10} s_4 \pi + 576 r^8 s_4^2 \pi^2 s_1^4 \\
 & - 6 r^8 s_2^2 s_1^2 s_3 - 10 r^8 s_2^2 s_1^2 s_3^2 + 1152 r^8 s_4^2 \pi^2 s_2^2 + 64 r^6 s_4 \pi s_1^4 - 8 r^6 s_1^3 s_3 s_2 - 8 r^6 s_1^3 s_2 s_3^2 + 1024 r^6 s_4^2 \pi^2 s_1^3 \\
 & - 16 r^6 s_2^2 s_1 s_3^2 + 64 r^6 s_2^2 s_1 s_3 + 112 r^4 s_4 \pi s_1^3 - 9 r^4 s_1^2 s_2 s_3^2 + 42 r^4 s_1^2 s_3 s_2 + 896 r^4 s_4^2 \pi^2 s_1^2 + 448 r^4 s_4^2 \pi^2 s_2 \\
 & + 96 r^2 s_4 \pi s_1^2 + 60 r^2 s_1 s_2 s_3^2 - 100 r^2 s_2 s_3 s_1 + 384 r^2 s_1 s_4^2 \pi^2 + 192 s_4^2 \pi^2 r^{20} s_2^5 + 32 s_4 \pi s_2^5 r^{18} + 12 s_2^3 r^{12} s_1^2 s_3 \\
 & + 8 s_2^4 r^{14} s_1 s_3 + 6 s_2^3 r^{12} s_1^2 s_3^2 + 4 s_2^4 r^{14} s_1 s_3^2 + 128 r^{10} s_4^2 \pi^2 s_1^5 + 8 r^{10} s_2^2 s_1^3 s_3 + 4 r^{10} s_2^2 s_1^3 s_3^2 + 16 r^8 s_4 \pi s_1^5 \\
 & + 2 r^8 s_1^4 s_3 s_2 + r^8 s_1^4 s_2 s_3^2 + 3 s_1^2 + 32 s_4 \pi s_1 + s_2^5 r^{16} + 16 s_1 r^2 s_2 + 32 r^6 s_2^2 s_1 - 4 r^4 s_1^4 s_3 - 3 r^4 s_1^4 s_3^2 + 19 r^4 s_2 s_1^2 \\
 & - 182 r^4 s_3 s_2^2 + 75 r^4 s_2^2 s_3^2 + 4 r^2 s_1^3 s_3 - 6 r^2 s_1^3 s_3^2 - 2 s_2^4 r^{12} s_3 - 3 s_2^4 r^{12} s_3^2 + 4 s_2^3 r^{10} s_1 + 4 r^8 s_2^2 s_1^2 - 25 r^8 s_2^3 s_3^2 \\
 & + 62 r^8 s_2^3 s_3 + 144 s_4 \pi s_2^4 r^{16} s_3 s_1 + 96 r^{10} s_4 \pi s_1^4 s_3 s_2 + 256 s_2^3 r^{14} s_4 \pi s_1^2 s_3 + 224 s_2^2 r^{12} s_4 \pi s_1^3 s_3 + 480 s_2^3 r^{12} s_4 \pi s_1 s_3 \\
 & + 640 s_2^2 r^{10} s_4 \pi s_1^2 s_3 + 352 r^8 s_4 \pi s_2 s_1^3 s_3 + 832 r^8 s_4 \pi s_2^2 s_1 s_3 + 640 r^6 s_4 \pi s_2 s_1^2 s_3 + 544 r^4 s_4 \pi s_1 s_2 s_3 \\
 & \left. + r^8 s_1^4 s_2 + 4 r^{10} s_1^3 s_2^2 + 2 s_2^5 r^{16} s_3 + s_2^5 r^{16} s_3^2 + 6 s_2^3 r^{12} s_1^2 + 4 s_2^4 r^{14} s_1 \right]. \tag{C}
 \end{aligned}$$

Appendix D

The adiabatic tangential index

$$\begin{aligned}
\Gamma_i = & - \left(-28 s_3 s_1^2 + 40 s_3 s_2 + 64 s_4^2 \pi^2 + 9 s_1^2 s_3^2 + 15 s_2^2 r^4 + s_2^4 r^{12} + 15 r^8 s_2^3 - r^4 s_1^4 + 2 r^2 s_1^3 + 3072 s_4^2 \pi^2 s_2^3 r^{14} s_1 \right. \\
& + 128 s_4 \pi s_2^4 r^{14} s_3 + 4224 s_2^2 r^{12} s_4^2 \pi^2 s_1^2 + 464 s_2^3 r^{12} s_4 \pi s_1 + 2560 s_2 r^{10} s_4^2 \pi^2 s_1^3 + 608 s_2^2 r^{10} s_4 \pi s_1^2 + 3840 s_2^2 r^{10} s_1 s_4^2 \pi^2 \\
& + 320 s_2^3 r^{10} s_4 \pi s_3 + 336 r^8 s_4 \pi s_2 s_1^3 + 3456 r^8 s_2 s_1^2 s_4^2 \pi^2 + 656 r^8 s_4 \pi s_2^2 s_1 + 64 r^6 s_4 \pi s_1^4 s_3 + 512 r^6 s_4 \pi s_2 s_1^2 \\
& + 2048 r^6 s_2 s_1 s_4^2 \pi^2 + 384 r^6 s_4 \pi s_2^2 s_3 + 128 r^4 s_4 \pi s_1^3 s_3 + 368 r^4 s_4 \pi s_1 s_2 + 128 r^2 s_4 \pi s_1^2 s_3 + 160 r^2 s_4 \pi s_2 s_3 \\
& + 1664 s_4^2 \pi^2 s_2^3 r^{16} s_1^2 + 896 s_4^2 \pi^2 s_2^4 r^{18} s_1 + 32 s_4 \pi s_2^5 r^{18} s_3 + 1536 s_2^2 r^{14} s_4^2 \pi^2 s_1^3 + 256 s_2^3 r^{14} s_4 \pi s_1^2 + 144 s_2^4 r^{16} s_4 \pi s_1 \\
& + 704 s_2 r^{12} s_4^2 \pi^2 s_1^4 + 224 s_2^2 r^{12} s_4 \pi s_1^3 + 96 r^{10} s_4 \pi s_2 s_1^4 + 16 r^8 s_4 \pi s_1^5 s_3 + 48 s_4 \pi s_1 s_3 + 96 s_4 \pi r^2 s_2 + 256 s_4 \pi r^6 s_2^2 \\
& + 832 s_4^2 \pi^2 r^{16} s_2^4 + 128 s_4 \pi s_2^4 r^{14} + 1408 s_2^3 r^{12} s_4^2 \pi^2 - 4 s_2^3 r^{10} s_1 s_3 - 8 s_2^3 r^{10} s_1 s_3^2 + 256 s_2^3 r^{10} s_4 \pi + 576 r^8 s_4^2 \pi^2 s_1^4 \\
& - 6 r^8 s_2^2 s_1^2 s_3 - 10 r^8 s_2^2 s_1^2 s_3^2 + 1152 r^8 s_4^2 \pi^2 s_2^2 + 64 r^6 s_4 \pi s_1^4 - 8 r^6 s_1^3 s_3 s_2 - 8 r^6 s_1^3 s_2 s_3^2 + 1024 r^6 s_4^2 \pi^2 s_1^3 \\
& - 16 r^6 s_2^2 s_1 s_3^2 + 64 r^6 s_2^2 s_1 s_3 + 112 r^4 s_4 \pi s_1^3 - 9 r^4 s_1^2 s_2 s_3^2 + 42 r^4 s_1^2 s_3 s_2 + 896 r^4 s_4^2 \pi^2 s_1^2 + 448 r^4 s_4^2 \pi^2 s_2 \\
& + 96 r^2 s_4 \pi s_1^2 + 60 r^2 s_1 s_2 s_3^2 - 100 r^2 s_2 s_3 s_1 + 384 r^2 s_1 s_4^2 \pi^2 + 192 s_4^2 \pi^2 r^{20} s_2^5 + 32 s_4 \pi s_2^5 r^{18} + 12 s_2^3 r^{12} s_1^2 s_3 \\
& + 8 s_2^4 r^{14} s_1 s_3 + 6 s_2^3 r^{12} s_1^2 s_3^2 + 4 s_2^4 r^{14} s_1 s_3^2 + 128 r^{10} s_4^2 \pi^2 s_1^5 + 8 r^{10} s_2^2 s_1^3 s_3 + 4 r^{10} s_2^2 s_1^3 s_3^2 + 16 r^8 s_4 \pi s_1^5 \\
& + 2 r^8 s_1^4 s_3 s_2 + r^8 s_1^4 s_2 s_3^2 + 3 s_1^2 + 32 s_4 \pi s_1 + s_2^5 r^{16} + 16 s_1 r^2 s_2 - 2 s_2^4 r^{12} s_3 - 3 s_2^4 r^{12} s_3^2 + 4 s_2^3 r^{10} s_1 + 4 r^8 s_2^2 s_1^2 \\
& - 25 r^8 s_2^3 s_3^2 + 62 r^8 s_2^3 s_3 + 32 r^6 s_2^2 s_1 - 4 r^4 s_1^4 s_3 - 3 r^4 s_1^4 s_3^2 + 19 r^4 s_2 s_1^2 - 182 r^4 s_3 s_2^2 + 75 r^4 s_2^2 s_3^2 + 4 r^2 s_1^3 s_3 \\
& - 6 r^2 s_1^3 s_3^2 + 144 s_4 \pi s_2^4 r^{16} s_3 s_1 + 96 r^{10} s_4 \pi s_1^4 s_3 s_2 + 256 s_2^3 r^{14} s_4 \pi s_1^2 s_3 + 224 s_2^2 r^{12} s_4 \pi s_1^3 s_3 + 480 s_2^3 r^{12} s_4 \pi s_1 s_3 \\
& + 640 s_2^2 r^{10} s_4 \pi s_1^2 s_3 + 352 r^8 s_4 \pi s_2 s_1^3 s_3 + 832 r^8 s_4 \pi s_2^2 s_1 s_3 + 640 r^6 s_4 \pi s_2 s_1^2 s_3 + 544 r^4 s_4 \pi s_1 s_2 s_3 + 4 s_2^4 r^{14} s_1 \\
& \left. + r^8 s_1^4 s_2 + 2 s_2^5 r^{16} s_3 + s_2^5 r^{16} s_3^2 + 6 s_2^3 r^{12} s_1^2 + 4 r^{10} s_2^2 s_1^3 \right) \left(12 s_1 + 20 s_2 r^2 + 32 s_4 \pi + 12 s_3 s_1 + 29 s_2^2 r^6 + s_2^4 r^{14} \right. \\
& + 10 r^{10} s_2^3 + r^6 s_1^4 + 8 r^4 s_1^3 + 19 r^2 s_1^2 + 256 s_4^2 \pi^2 s_2^3 r^{16} s_1 + 16 s_4 \pi s_2^4 r^{16} s_3 + 384 s_2^2 r^{14} s_4^2 \pi^2 s_1^2 + 64 s_2^3 r^{14} s_4 \pi s_1 \\
& + 256 s_2 r^{12} s_4^2 \pi^2 s_1^3 + 96 s_2^2 r^{12} s_4 \pi s_1^2 + 768 s_2^2 r^{12} s_1 s_4^2 \pi^2 + 112 s_2^3 r^{12} s_4 \pi s_3 + 64 r^{10} s_4 \pi s_2 s_1^3 + 768 r^{10} s_2 s_1^2 s_4^2 \pi^2 \\
& + 320 r^{10} s_4 \pi s_2^2 s_1 + 16 r^8 s_4 \pi s_1^4 s_3 + 304 r^8 s_4 \pi s_2 s_1^2 + 768 r^8 s_2 s_1 s_4^2 \pi^2 + 176 r^8 s_4 \pi s_2^2 s_3 + 80 r^6 s_4 \pi s_1^3 s_3 \\
& + 384 r^6 s_4 \pi s_1 s_2 + 112 r^4 s_4 \pi s_1^2 s_3 + 80 r^4 s_4 \pi s_2 s_3 + 48 r^2 s_4 \pi s_1 s_3 + 144 s_4 \pi r^4 s_2 + 128 s_4 \pi r^2 s_1 + 208 s_4 \pi r^8 s_2^2 \\
& + 64 s_4^2 \pi^2 r^{18} s_2^4 + 16 s_4 \pi s_2^4 r^{16} + 256 s_2^3 r^{14} s_4^2 \pi^2 + 8 s_2^3 r^{12} s_1 s_3 + 4 s_2^3 r^{12} s_1 s_3^2 + 112 s_2^3 r^{12} s_4 \pi + 64 r^{10} s_4^2 \pi^2 s_1^4 \\
& + 12 r^{10} s_2^2 s_1^2 s_3 + 6 r^{10} s_2^2 s_1^2 s_3^2 + 384 r^{10} s_4^2 \pi^2 s_2^2 + 16 r^8 s_4 \pi s_1^4 + 8 r^8 s_1^3 s_3 s_2 + 4 r^8 s_1^3 s_2 s_3^2 + 256 r^8 s_4^2 \pi^2 s_1^3 \\
& + 26 r^8 s_2^2 s_1 s_3^2 + 42 r^8 s_2^2 s_1 s_3 + 96 r^6 s_4 \pi s_1^3 + 22 r^6 s_1^2 s_2 s_3^2 + 36 r^6 s_1^2 s_3 s_2 + 384 r^6 s_4^2 \pi^2 s_1^2 + 256 r^6 s_4^2 \pi^2 s_2 \\
& + 176 r^4 s_4 \pi s_1^2 + 30 r^4 s_1 s_2 s_3^2 + 26 r^4 s_2 s_3 s_1 + 256 r^4 s_1 s_4^2 \pi^2 + 40 s_3 r^2 s_2 + 48 s_1 r^4 s_2 + 2 s_2^4 r^{14} s_3 + s_2^4 r^{14} s_3^2 + 4 s_2^3 r^{12} s_1 \\
& + 6 r^{10} s_2^2 s_1^2 + 10 r^{10} s_2^3 s_3^2 + 16 r^{10} s_2^3 s_3 + 4 r^8 s_1^3 s_2 + 28 r^8 s_2^2 s_1 + 2 r^6 s_1^4 s_3 + r^6 s_1^4 s_3^2 + 26 r^6 s_2 s_1^2 + 6 r^6 s_3 s_2^2 \\
& + 25 r^6 s_2^2 s_3^2 + 10 r^4 s_1^3 s_3 + 6 r^4 s_1^3 s_3^2 + 8 r^2 s_3 s_1^2 + 9 r^2 s_1^2 s_3^2 + 64 r^2 s_4^2 \pi^2 + 64 s_2^3 r^{14} s_4 \pi s_1 s_3 + 96 s_2^2 r^{12} s_4 \pi s_1^2 s_3 \\
& \left. + 64 r^{10} s_4 \pi s_2 s_1^3 s_3 + 304 r^{10} s_4 \pi s_2^2 s_1 s_3 + 272 r^8 s_4 \pi s_2 s_1^2 s_3 + 288 r^6 s_4 \pi s_1 s_2 s_3 \right) \left\{ 4 \left(12 s_2^2 r^4 + 3 r^6 s_2^2 s_1 + r^8 s_2^3 \right. \right. \\
& \left. \left. + 13 s_1 r^2 s_2 + 3 r^4 s_2 s_1^2 - 5 s_2 + 5 s_1^2 + r^2 s_1^3 \right) \left(32 s_4 \pi + 12 s_3 s_1 + 5 s_2^2 r^6 + s_2^4 r^{14} + 6 r^{10} s_2^3 + r^6 s_1^4 + 4 r^4 s_1^3 + 3 r^2 s_1^2 \right. \right. \\
& + 256 s_4^2 \pi^2 s_2^3 r^{16} s_1 + 16 s_4 \pi s_2^4 r^{16} s_3 + 384 s_2^2 r^{14} s_4^2 \pi^2 s_1^2 + 64 s_2^3 r^{14} s_4 \pi s_1 + 256 s_2 r^{12} s_4^2 \pi^2 s_1^3 + 96 s_2^2 r^{12} s_4 \pi s_1^2 \\
& + 768 s_2^2 r^{12} s_1 s_4^2 \pi^2 + 112 s_2^3 r^{12} s_4 \pi s_3 + 64 r^{10} s_4 \pi s_2 s_1^3 + 768 r^{10} s_2 s_1^2 s_4^2 \pi^2 + 320 r^{10} s_4 \pi s_2^2 s_1 + 16 r^8 s_4 \pi s_1^4 s_3 \\
& + 304 r^8 s_4 \pi s_2 s_1^2 + 768 r^8 s_2 s_1 s_4^2 \pi^2 + 176 r^8 s_4 \pi s_2^2 s_3 + 80 r^6 s_4 \pi s_1^3 s_3 + 384 r^6 s_4 \pi s_1 s_2 + 112 r^4 s_4 \pi s_1^2 s_3 + 80 r^4 s_4 \pi s_2 s_3 \\
& + 48 r^2 s_4 \pi s_1 s_3 + 144 s_4 \pi r^4 s_2 + 128 s_4 \pi r^2 s_1 + 208 s_4 \pi r^8 s_2^2 + 64 s_4^2 \pi^2 r^{18} s_2^4 + 16 s_4 \pi s_2^4 r^{16} + 256 s_2^3 r^{14} s_4^2 \pi^2 \\
& + 8 s_2^3 r^{12} s_1 s_3 + 4 s_2^3 r^{12} s_1 s_3^2 + 112 s_2^3 r^{12} s_4 \pi + 64 r^{10} s_4^2 \pi^2 s_1^4 + 12 r^{10} s_2^2 s_1^2 s_3 + 6 r^{10} s_2^2 s_1^2 s_3^2 + 384 r^{10} s_4^2 \pi^2 s_2^2 \\
& + 16 r^8 s_4 \pi s_1^4 + 8 r^8 s_1^3 s_3 s_2 + 4 r^8 s_1^3 s_2 s_3^2 + 256 r^8 s_4^2 \pi^2 s_1^3 + 26 r^8 s_2^2 s_1 s_3^2 + 42 r^8 s_2^2 s_1 s_3 + 96 r^6 s_4 \pi s_1^3 + 22 r^6 s_1^2 s_2 s_3^2 \\
& + 36 r^6 s_1^2 s_3 s_2 + 384 r^6 s_4^2 \pi^2 s_1^2 + 256 r^6 s_4^2 \pi^2 s_2 + 176 r^4 s_4 \pi s_1^2 + 30 r^4 s_1 s_2 s_3^2 + 26 r^4 s_2 s_3 s_1 + 256 r^4 s_1 s_4^2 \pi^2 \\
& + 40 s_3 r^2 s_2 + 8 s_1 r^4 s_2 + 2 s_2^4 r^{14} s_3 + s_2^4 r^{14} s_3^2 + 4 s_2^3 r^{12} s_1 + 6 r^{10} s_2^2 s_1^2 + 10 r^{10} s_2^3 s_3^2 + 16 r^{10} s_2^3 s_3 + 4 r^8 s_1^3 s_2 \\
& + 16 r^8 s_2^2 s_1 + 2 r^6 s_1^4 s_3 + r^6 s_1^4 s_3^2 + 14 r^6 s_2 s_1^2 + 6 r^6 s_3 s_2^2 + 25 r^6 s_2^2 s_3^2 + 10 r^4 s_1^3 s_3 + 6 r^4 s_1^3 s_3^2 + 8 r^2 s_3 s_1^2 \\
& \left. + 9 r^2 s_1^2 s_3^2 + 64 r^2 s_4^2 \pi^2 + 64 s_2^3 r^{14} s_4 \pi s_1 s_3 + 96 s_2^2 r^{12} s_4 \pi s_1^2 s_3 + 64 r^{10} s_4 \pi s_2 s_1^3 s_3 + 304 r^{10} s_4 \pi s_2^2 s_1 s_3 \right\}
\end{aligned}$$

$$+272 r^8 s_4 \pi s_2 s_1^2 s_3 + 288 r^6 s_4 \pi s_1 s_2 s_3 \left. \right) (1 + s_1 r^2 + s_2 r^4) \left. \right\}^{-1}. \quad (\text{D})$$

Data availability

The data underlying this article will be shared on any reasonable request to the corresponding author.

REFERENCES

- Ade, P. A. R., et al. 2016, *Astron. Astrophys.*, 594, doi: [10.1051/0004-6361/201525830](https://doi.org/10.1051/0004-6361/201525830)
- Albrecht, A., & Steinhardt, P. J. 1982, *Phys. Rev. Lett.*, 48, 1220, doi: [10.1103/PhysRevLett.48.1220](https://doi.org/10.1103/PhysRevLett.48.1220)
- Astashenok, A. V., Capozziello, S., Odintsov, S. D., & Oikonomou, V. K. 2021, *Phys. Lett. B*, 816, 136222, doi: [10.1016/j.physletb.2021.136222](https://doi.org/10.1016/j.physletb.2021.136222)
- Böhmer, C. G., & Harko, T. 2006, *Classical and Quantum Gravity*, 23, 6479, doi: [10.1088/0264-9381/23/22/023](https://doi.org/10.1088/0264-9381/23/22/023)
- Bowers, R. L., & Liang, E. 1974, *Astrophys. J.*, 188, 657, doi: [10.1086/152760](https://doi.org/10.1086/152760)
- Canuto, V. 1974, *Annual Review of Astronomy and Astrophysics*, 12, 167
- Capozziello, S., & De Laurentis, M. 2011, *Phys. Rept.*, 509, 167, doi: [10.1016/j.physrep.2011.09.003](https://doi.org/10.1016/j.physrep.2011.09.003)
- Capozziello, S., Lobo, F. S. N., & Mimoso, J. P. 2014, *Phys. Lett. B*, 730, 280, doi: [10.1016/j.physletb.2014.01.066](https://doi.org/10.1016/j.physletb.2014.01.066)
- . 2015, *Phys. Rev. D*, 91, 124019, doi: [10.1103/PhysRevD.91.124019](https://doi.org/10.1103/PhysRevD.91.124019)
- Capozziello, S., Matsumoto, J., Nojiri, S., & Odintsov, S. D. 2010, *Phys. Lett. B*, 693, 198, doi: [10.1016/j.physletb.2010.08.030](https://doi.org/10.1016/j.physletb.2010.08.030)
- Chaichian, M., Kluson, J., Oksanen, M., & Tureanu, A. 2014, *JHEP*, 12, 102, doi: [10.1007/JHEP12\(2014\)102](https://doi.org/10.1007/JHEP12(2014)102)
- Chamseddine, A. H., & Mukhanov, V. 2013, *JHEP*, 11, 135, doi: [10.1007/JHEP11\(2013\)135](https://doi.org/10.1007/JHEP11(2013)135)
- . 2017a, *JCAP*, 1703, 009, doi: [10.1088/1475-7516/2017/03/009](https://doi.org/10.1088/1475-7516/2017/03/009)
- . 2017b, *Eur. Phys. J.*, 183, doi: [10.1140/epjc/s10052-017-4759-z](https://doi.org/10.1140/epjc/s10052-017-4759-z)
- . 2018, *JHEP*, 06, 060, doi: [10.1007/JHEP06\(2018\)060](https://doi.org/10.1007/JHEP06(2018)060)
- Chamseddine, A. H., Mukhanov, V., & Vikman, A. 2014, *JCAP*, 1406, 017, doi: [10.1088/1475-7516/2014/06/017](https://doi.org/10.1088/1475-7516/2014/06/017)
- Chan, R., Herrera, L., & Santos, N. O. 1993, *Monthly Notices of the Royal Astronomical Society*, 265, 533, doi: [10.1093/mnras/265.3.533](https://doi.org/10.1093/mnras/265.3.533)
- Chandrasekhar, S. 1964, *ApJ*, 140, 417, doi: [10.1086/147938](https://doi.org/10.1086/147938)
- Das, S., Ray, S., Khlopov, M., Nandi, K. K., & Parida, B. K. 2021, <https://arxiv.org/abs/2102.07099>
- De Felice, A., & Tsujikawa, S. 2010, *Living Rev. Rel.*, 13, 3, doi: [10.12942/lrr-2010-3](https://doi.org/10.12942/lrr-2010-3)
- Deb, D., Chowdhury, S. R., Ray, S., Rahaman, F., & Guha, B. K. 2017, *Annals Phys.*, 387, 239, doi: [10.1016/j.aop.2017.10.010](https://doi.org/10.1016/j.aop.2017.10.010)
- Deb, D., Roy Chowdhury, S., Ray, S., & Rahaman, F. 2018, *Gen. Rel. Grav.*, 50, 112, doi: [10.1007/s10714-018-2434-9](https://doi.org/10.1007/s10714-018-2434-9)
- Deruelle, N., & Rua, J. 2014, *JCAP*, 1409, 002, doi: [10.1088/1475-7516/2014/09/002](https://doi.org/10.1088/1475-7516/2014/09/002)
- Domnech, G., Mukohyama, S., Namba, R., et al. 2015, *Phys. Rev.*, 084027, doi: [10.1103/PhysRevD.92.084027](https://doi.org/10.1103/PhysRevD.92.084027)
- El Hanafy, W., & Nashed, G. G. L. 2016, *Astrophys. Space Sci.*, 361, 68, doi: [10.1007/s10509-016-2662-y](https://doi.org/10.1007/s10509-016-2662-y)
- Firouzjahi, H., Gorji, M. A., Hosseini Mansoori, S. A., Karami, A., & Rostami, T. 2018, *JCAP*, 11, 046, doi: [10.1088/1475-7516/2018/11/046](https://doi.org/10.1088/1475-7516/2018/11/046)
- Gangopadhyay, T., Ray, S., Li, X.-D., Dey, J., & Dey, M. 2013, *Mon. Not. Roy. Astron. Soc.*, 431, 3216, doi: [10.1093/mnras/stt401](https://doi.org/10.1093/mnras/stt401)
- Gao, C., Gong, Y., Wang, X., & Chen, X. 2011, *Phys. Lett. B*, 702, 107, doi: [10.1016/j.physletb.2011.06.085](https://doi.org/10.1016/j.physletb.2011.06.085)
- Geng, C.-Q., Hossain, M. W., Myrzakulov, R., Sami, M., & Saridakis, E. N. 2015, *Phys. Rev. D*, 92, 023522, doi: [10.1103/PhysRevD.92.023522](https://doi.org/10.1103/PhysRevD.92.023522)
- Gorji, M. A., Allahyari, A., Khodadi, M., & Firouzjahi, H. 2020, *Phys. Rev. D*, 101, 124060, doi: [10.1103/PhysRevD.101.124060](https://doi.org/10.1103/PhysRevD.101.124060)
- Guth, A. H. 1981, *Phys. Rev. D*, 23, 347, doi: [10.1103/PhysRevD.23.347](https://doi.org/10.1103/PhysRevD.23.347)
- Guth, A. H., & Pi, S. Y. 1982, *Phys. Rev. Lett.*, 49, 1110, doi: [10.1103/PhysRevLett.49.1110](https://doi.org/10.1103/PhysRevLett.49.1110)
- Harrison, B. K., Thorne, K. S., Wakano, M., & Wheeler, J. A. 1965, *Gravitation Theory and Gravitational Collapse*
- Hawking, S. W. 1982, *Phys. Lett. B*, 115, 295, doi: [10.1016/0370-2693\(82\)90373-2](https://doi.org/10.1016/0370-2693(82)90373-2)
- Heintzmann, H., & Hillebrandt, W. 1975, *aap*, 38, 51
- Herrera, L. 1992, *Physics Letters A*, 165, 206, doi: [https://doi.org/10.1016/0375-9601\(92\)90036-L](https://doi.org/10.1016/0375-9601(92)90036-L)
- Herrera, L., & Santos, N. O. 1997, *Physics Reports*, 286, 53
- Hossain, M. W., Myrzakulov, R., Sami, M., & Saridakis, E. N. 2014, *Phys. Rev. D*, 89, 123513, doi: [10.1103/PhysRevD.89.123513](https://doi.org/10.1103/PhysRevD.89.123513)
- Huang, Q.-G., Wang, K., & Wang, S. 2016, *Phys. Rev. D*, 93, 103516, doi: [10.1103/PhysRevD.93.103516](https://doi.org/10.1103/PhysRevD.93.103516)
- Ivanov, B. V. 2002, *Physical Review D*, 65, 104011
- Kalam, M., Rahaman, F., Ray, S., et al. 2012, *The European Physical Journal C*, 72, 1
- Lim, E. A., Sawicki, I., & Vikman, A. 2010, *JCAP*, 05, 012, doi: [10.1088/1475-7516/2010/05/012](https://doi.org/10.1088/1475-7516/2010/05/012)
- Linde, A. D. 1982, *Phys. Lett. B*, 108, 389, doi: [10.1016/0370-2693\(82\)91219-9](https://doi.org/10.1016/0370-2693(82)91219-9)

- Martin, J., Ringeval, C., Trotta, R., & Vennin, V. 2014a, *Journal of Cosmology and Astroparticle Physics*, 2014, 039
- Martin, J., Ringeval, C., & Vennin, V. 2014b, *Phys. Dark Univ.*, 5-6, 75, doi: [10.1016/j.dark.2014.01.003](https://doi.org/10.1016/j.dark.2014.01.003)
- Maurya, S., Banerjee, A., & Hansraj, S. 2018, *Physical Review D*, 97, 044022
- Maurya, S. K., Gupta, Y. K., Ray, S., & Deb, D. 2016, *Eur. Phys. J. C*, 76, 693, doi: [10.1140/epjc/s10052-016-4527-5](https://doi.org/10.1140/epjc/s10052-016-4527-5)
- Merafina, M., & Ruffini, R. 1989, *aap*, 221, 4
- Mukhanov, V. F., & Chibisov, G. V. 1981, *JETP Lett.*, 33, 532
- Nashed, G. G. L. 2002, *Nuovo Cim. B*, 117, 521.
<https://arxiv.org/abs/gr-qc/0109017>
- . 2007, *Mod. Phys. Lett. A*, 22, 1047,
doi: [10.1142/S021773230702141X](https://doi.org/10.1142/S021773230702141X)
- Nojiri, S., & Odintsov, S. D. 2011, *Phys. Rept.*, 505, 59,
doi: [10.1016/j.physrep.2011.04.001](https://doi.org/10.1016/j.physrep.2011.04.001)
- Nojiri, S., Odintsov, S. D., & Oikonomou, V. K. 2017, *Phys. Rept.*, 692, 1, doi: [10.1016/j.physrep.2017.06.001](https://doi.org/10.1016/j.physrep.2017.06.001)
- Oppenheimer, J. R., & Volkoff, G. M. 1939, *Phys. Rev.*, 55, 374,
doi: [10.1103/PhysRev.55.374](https://doi.org/10.1103/PhysRev.55.374)
- Özel, F., Psaltis, D., Güver, T., et al. 2016, *apj*, 820, 28,
doi: [10.3847/0004-637X/820/1/28](https://doi.org/10.3847/0004-637X/820/1/28)
- Perlmutter, S., et al. 1999, *Astrophys. J.*, 517, 565,
doi: [10.1086/307221](https://doi.org/10.1086/307221)
- Ponce de Leon, J. 1993, *General Relativity and Gravitation*, 25, 1123, doi: [10.1007/BF00763756](https://doi.org/10.1007/BF00763756)
- Rahaman, F., Sharma, R., Ray, S., Maulick, R., & Karar, I. 2012, *Eur. Phys. J. C*, 72, 2071, doi: [10.1140/epjc/s10052-012-2071-5](https://doi.org/10.1140/epjc/s10052-012-2071-5)
- Riess, A. G., et al. 1998, *Astron. J.*, 116, 1009,
doi: [10.1086/300499](https://doi.org/10.1086/300499)
- . 2004, *Astrophys. J.*, 607, 665, doi: [10.1086/383612](https://doi.org/10.1086/383612)
- Roupas, Z., & Nashed, G. G. L. 2020, *Eur. Phys. J. C*, 80, 905,
doi: [10.1140/epjc/s10052-020-08462-1](https://doi.org/10.1140/epjc/s10052-020-08462-1)
- Ruderman, M. 1972, *Ann. Rev. Astron. Astrophys.*, 10, 427,
doi: [10.1146/annurev.aa.10.090172.002235](https://doi.org/10.1146/annurev.aa.10.090172.002235)
- Sebastiani, L., Vagnozzi, S., & Myrzakulov, R. 2017, *Adv. High Energy Phys.*, 2017, 3156915, doi: [10.1155/2017/3156915](https://doi.org/10.1155/2017/3156915)
- Shee, D., Rahaman, F., Guha, B. K., & Ray, S. 2016, *Astrophys. Space Sci.*, 361, 167, doi: [10.1007/s10509-016-2753-9](https://doi.org/10.1007/s10509-016-2753-9)
- Shen, L., Zheng, Y., & Li, M. 2019, *JCAP*, 12, 026,
doi: [10.1088/1475-7516/2019/12/026](https://doi.org/10.1088/1475-7516/2019/12/026)
- Singh, K. N., Rahaman, F., & Banerjee, A. 2019.
<https://arxiv.org/abs/1909.10882>
- Starobinsky, A. A. 1982, *Phys. Lett. B*, 117, 175,
doi: [10.1016/0370-2693\(82\)90541-X](https://doi.org/10.1016/0370-2693(82)90541-X)
- Tolman, R. C. 1939, *Phys. Rev.*, 55, 364,
doi: [10.1103/PhysRev.55.364](https://doi.org/10.1103/PhysRev.55.364)
- Varela, V., Rahaman, F., Ray, S., Chakraborty, K., & Kalam, M. 2010, *Phys. Rev. D*, 82, 044052,
doi: [10.1103/PhysRevD.82.044052](https://doi.org/10.1103/PhysRevD.82.044052)
- Zeldovich, Y. B., & Novikov, I. D. 1971, *Relativistic astrophysics. Vol.1: Stars and relativity*

